

METAKARYOTIC BIOLOGY: NOVEL GENOMIC ORGANIZATION IN  
HUMAN STEM-LIKE CELLS OF FETAL-JUVENILE DEVELOPMENT  
AND CARCINOGENESIS

by  
Amanda Natalie Gruhl

B.S. Biology  
Massachusetts Institute of Technology, 1999

Submitted to the Department of Biological Engineering in Partial Fulfillment  
of the Requirements for the Degree of

Doctor of Philosophy in Genetic Toxicology  
at the  
Massachusetts Institute of Technology

June 2008

© 2008 Massachusetts Institute of Technology. All rights reserved.

Signature of Author: \_\_\_\_\_

Department of Biological Engineering  
May 22, 2008

Certified by: \_\_\_\_\_

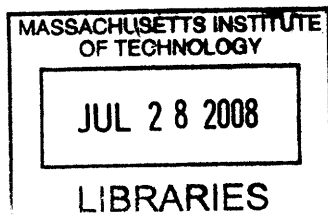
William G. Thilly  
Professor, Department of Biological Engineering  
Thesis Advisor

Certified by: \_\_\_\_\_

Elena V. Gostjeva  
Visiting Research Scientist, Department of Biological Engineering  
Senior Research Scientist, Institute of Agriculture and Biotechnology, Kiev, Ukraine  
Thesis Advisor

Accepted by: \_\_\_\_\_

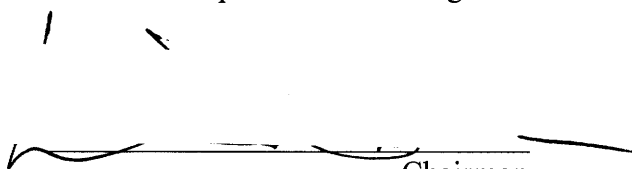
Alan J. Grodzinsky  
Professor, Department of Electrical, Mechanical, and Biological Engineering  
Chairman, Division Committee on Graduate Studies



ARCHIVES

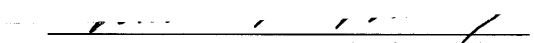
This doctoral thesis has been examined by a Committee of the Department of Biological Engineering as follows:

Professor Leona D. Samson



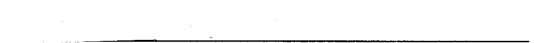
Chairman

Professor William G. Thilly



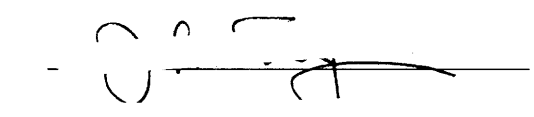
Thesis Advisor

Dr. Elena V. Gostjeva



Thesis Advisor


Professor John M. Essigmann



Professor Bevin P. Engelward



Dr. Thomas R. Skopek



# METAKARYOTIC BIOLOGY: NOVEL GENOMIC ORGANIZATION IN HUMAN STEM-LIKE CELLS OF FETAL-JUVENILE DEVELOPMENT AND CARCINOGENESIS

by Amanda N. Gruhl

Submitted to the Department of Biological Engineering on May 22, 2008 in Partial Fulfillment of the Requirements for the Degree of Doctor of Philosophy in Genetic Toxicology

## ABSTRACT

Eight distinct nuclear shapes, or morphologies, have been discovered in human proto-organs and tumors, including bell-shaped nuclei with stem-like properties. These bell-shaped, or “metakaryotic,” nuclei are abundant in fetal tissues and neoplasias, but rare in normal adult somatic tissues. Metakaryotic nuclei employ an unusual process for division in which DNA synthesis, partial genomic condensation, and separation of the two nuclei in a cup-from-cup fashion occur concurrently, as shown by Feulgen densitometry and single-stranded DNA assays by Dr. Elena Gostjeva. This is clearly different from the sequential steps of S-phase DNA synthesis, chromatin condensation, chromosomal separation, and genomic segregation that occur in mitotic eukaryotic cells. In order to discover how a genome apparently devoid of chromosomes might be organized, this thesis focused on recognizable DNA sequences common to all chromosomes: centromeres and telomeres. Fluorescence In Situ Hybridization (FISH) with pan-centromeric and pan-telomeric probes was applied to samples of human tissue. (A collaborating lab used centromeric and telomeric antibodies to confirm results.) An optimized FISH protocol was developed specifically for metakaryotic nuclei and tested in both human cell lines and eukaryotic cells as experimental controls. Staining of metakaryotic nuclei resulted in approximately 23 centromeric regions in each, unlike the expected number of 46 regions seen in eukaryotic nuclei. Many of these staining regions contained paired centromere signals, or doublets. This suggested a genomic organization of homologous chromosomes paired at their centromere regions. If this were the case, one would expect 46 telomeric signals per nuclei, if telomeres were also homologously paired. Unexpectedly, an average of 23 telomeric regions were found in many, if not all, bell-shaped metakaryotic nuclei. This, along with the observation of a condensed double ring around the mouth of the bell-shaped nuclei, suggested the possibility of a genome organized as paired, continuous genomic circles. Studies of telomere joining in metakaryotic nuclei by Dr. Per Olaf Ekstrøm have provided further evidence for the paired genomic circle model. The results in this thesis are an original contribution to the field of stem cell physiology, a starting point for further investigation of DNA organization, synthesis, and repair in these metakaryotic cells, and hopefully will lead to a greater understanding of human development, growth, and cancer.

Thesis Advisor: William G. Thilly  
Title: Professor, Division of Biological Engineering  
Thesis Advisor: Dr. Elena Gostjeva  
Title: Visiting Research Scientist, Department of Biological Engineering;  
Senior Research Scientist, Institute of Agriculture and Biotechnology,  
Kiev, Ukraine

## ACKNOWLEDGEMENTS

I would like to first thank my thesis advisors, Professor William G. Thilly and Dr. Elena Gostjeva for their unending patience, support, and guidance during my graduate school career. Indeed, Dr. Gostjeva's work was what made my thesis possible, as it was instrumental in planning, executing, and discussing my own work. I am honored to have worked with her and thankful that she allowed me to present her discoveries in this thesis. Professor Thilly has been an academic advisor of mine since I was a undergraduate at MIT and started me right away doing my own projects to learn autonomy. He was always truthful and straightforward about all matters, and I am thankful for his insights, and push in the right direction when necessary. Professor Thilly and Dr. Gostjeva went above and beyond as advisors, and not only helped me through my academic struggles, but many of my personal ones as well, and I thank them again for everything they did on my behalf.

I sincerely thank my committee members, Professor Leona Samson, Professor John Essigmann, Professor Bevin Engelward, Dr. Thomas Skopek, and Professor Alec Morley for their invaluable comments and suggestions. I particularly would like to thank Professor Samson for taking over as Chairman of my committee during the later stages of my thesis.

I am thankful to Professor Firouz Darroudi for setting up experiments in his own lab specifically to test several of my major findings, and for allowing his results to be presented in this thesis as a confirmation of my findings. His correspondence was also extremely helpful in discussing my results. I would also like to thank Dr. Per Olaf Ekstrøm for sharing his results with me and allowing me to present his work as derived from my findings. His insights about telomere joining and life in the Thilly Lab were much appreciated.

I would like to thank Mr. Michael Hallacy and Ms. Christine Burnitz for their constant help and support with our lab microscopes, and to Mrs. Rita DeMeo, who has been indispensable both personally and professionally. I thank Mrs. Dalia Fares and the rest of the Biological Engineering administrative staff for their patience and help with all administrative issues. Thank you so much to all the present and past members of the Thilly and Sherley Labs I have been fortunate enough to know and spend time with over the last 13 years. They provided me with training, advice, and an ear when I needed it. Thank you all.

I thank all of my friends for their love and support, particularly Mr. Shawn Hershey, Mr. Ogden Sawyer, and Mrs. Erin Sawyer who helped me through my struggles, rejoiced in my successes, and were always there when I needed them. Finally, I would like to thank my family for their constant love and support, and I dedicate this thesis to them:

To my brother, Steven, who has constant faith in my abilities. To my mother, Nancy, who is always there to listen and advise wisely, especially on the lessons of life. To my father, James, my first teacher, who inspired me to take this journey, and to never stop learning.

## TABLE OF CONTENTS

Title Page	1
Committee Page	2
Abstract	3
Acknowledgements	4
Table of Contents	5
List of Figures	8
List of Tables	10
List of Abbreviations	11
1. Introduction	12
2. Background	12
2.1 Eukaryotic Mitotic Human Cells: Basic DNA Organization and Nuclear Structures	12
2.1.1 Chromosomes	12
2.1.2 Centromeres	15
2.1.3 Telomeres	15
2.2 Nuclear Organization of Eukaryotic Cells	18
2.2.1 Nuclear Organization of Eukaryotic Cells in Mammals	18
2.2.1.1 Interphase	18
2.2.1.2 Mitosis	22
2.2.1.3 Meiosis and Gametogenesis	22
2.2.2 Nuclear Organization in Other Species	24
2.3 Metakaryotic Cells	28

2.3.1 Basic Structure and Developmental Stages	28
2.3.2 Metakaryotes and Carcinogenesis	33
2.3.3 Amitotic Division of Metakaryotes	33
3. Materials and Methods	36
3.1 TK6 Cell Lines	36
3.2 Tissue sources and preparation	36
3.3 Slide preparation	36
3.3.1 TK6 Cells	36
3.3.1.1 TK6 Karyotypes	37
3.3.1.2 TK6 FISH Controls and Optimization Trials	37
3.3.2 Tissues	37
3.4 Fluorescence In Situ Hybridization (FISH)	37
3.4.1 Positive TK6 FISH controls	38
3.4.2 TK6 and Tissue Whole Chromosome Probe FISH Protocol	38
3.4.3 TK6 and Tissue Centromeric/Telomeric FISH Protocol	38
3.5 Imaging	39
3.5.1 Microscopy	39
3.5.2 Image analysis	39
4. Results	40
4.1 Controls	40
4.1.1 Centromere Counts	40
4.1.1.1 Human Lymphoblastoid Cell Line (TK6)	40
4.1.1.2 Human Fetal Gut and Spinal Cord	43

4.1.2 Telomere Counts	43
4.1.2.1 Human Fetal Gut and Spinal Cord	43
4.1.3 Whole Chromosomes	43
4.1.3.1 Human Lymphoblastoid Cell Line (TK6)	43
4.1.3.2 Human Fetal Gut	43
4.2 Metakaryotic Cells	44
4.2.1 Centromeres	44
4.2.1.1 Human Fetal Gut and Spinal Cord	44
4.2.1.2 Human Colon FAPC Adenomas and Adenocarcinomas	44
4.2.2 Telomere Counts	47
4.2.2.1 Human Fetal Gut and Spinal Cord	47
4.2.3 Whole Chromosomes	47
4.2.3.1 Human Fetal Gut	47
4.3 Statistics	49
4.4 Sources of Error	51
5. Discussion	52
5.1 Control Results	52
5.2 Metakaryotic Centromere and Telomere Organization	52
5.3 Metakaryotic Genome Models and Additional Findings	55
5.4 Related Studies	58
5.5 Mutation in Metakaryotes from Human Development	62
Conclusion	65
References	66

## LIST OF FIGURES

Figure 1: Theories of DNA and chromosome structures.	14
Figure 2: G-quadruplex structures of the human telomere repeat sequence.	17
Figure 3: Model of interphase nuclear architecture.	21
Figure 4: Centromere and telomere organization in mouse and human meiosis.	25
Figure 5. Telomere associations in human sperm cells.	26
Figure 6. Telomere localization in human sperm cells.	27
Figure 7: Distribution of bell-shaped nuclei in human fetal proto-organs and other organisms.	29
Figure 8: Metakaryotic cells in syncytia from human fetal gut at 5-7 weeks.	30
Figure 9: Extrasyncytial metakaryotic cells from human fetal intestine at 13 weeks.	31
Figure 10: Metakaryotic cells in normal human adult colon tissue.	32
Figure 11: Metakaryotic division processes.	34
Figure 12: Asymmetric amitotic division of human metakaryotic nuclei and mitotic division of other nuclear morphotypes.	35
Figure 13: Pan-centromeric FISH staining of TK6 mitotic figures.	42
Figure 14: FISH staining of human centromeric regions in single and dividing metakaryotic nuclei.	45
Figure 15: Counts of centromeric and telomeric staining regions in single, extrasyncytial, fetal metakaryotic nuclei.	46
Figure 16: FISH staining of chromosome 6 in 12 week human fetal gut.	48
Figure 17: Confirmation of FISH results using antibody staining of human centromeric and telomeric regions in metakaryotic cells.	54
Figure 18: Possible models for metakaryotic genomic organization.	56
Figure 19: Model for possible homologous pairing of chromosome 6 in metakaryotes.	57



Figure 20: Capillary electrophoresis results from telomere bridging PCR studies by Dr. Per Olaf Ekstrøm using peritelomeric primers.	59
Figure 21: Model of human telomere bridging by Dr. Per Olaf Ekstrøm.	60
Figure 22: Single stranded DNA studies on dividing metakaryotic nuclei conducted by Dr. Elena Gostjeva.	61
Figure 23: Lung mutant fractions as a function of smoking status and age.	63
Figure 24: Analyses of lung mutant cluster numbers and sizes in mitochondrial and nuclear DNA.	64

## LIST OF TABLES

Table 1: TK6 culture karyotypes by Dr. Anne Higgins at Brigham and Women's Hospital.	41
Table 2: FISH centromeric and telomeric staining counts and statistics.	50

## LIST OF ABBREVIATIONS

APC	Adenomatous Polyposis Coli
bp	basepair
CCD	Charge-coupled device
CENP	Centromere proteins
CT	Chromosomal territory
DAPI	4', 6-diamidino-2-phenylindole
DMSO	Dimethyl sulfoxide
DOP-PCR	Degenerated oligonucleotide primed PCR
DTT	Dithiothreitol
FAPC	Familial Adenomatous Polyposis Coli
FISH	Fluorescence in situ hybridization
FITC	Fluorescein isothiocyanate
IOD	Integrated optical density
PBD	Phosphate buffer detergent
PCR	Polymerase chain reaction
SC	Synaptonemal complex
SSC	Saline sodium citrate
TEBP	Telomere end-binding proteins
TERT	Telomere reverse transcriptases

## 1. INTRODUCTION

In September 2003, Dr. Elena V. Gostjeva found a new type of cell in human proto-organs and tumors she dubbed the "metakaryotic" cell. Her findings underlie this thesis, and include the following discoveries to date. This cell has a peculiar bell-shaped nucleus, and an amitotic division process that is concurrent with DNA synthesis. It undergoes symmetric and asymmetric division into different cell types (the only cell ever observed to do so *in vivo*), and it is abundant in fetal, adenomatous, adenocarcinomatous and metastatic tissues, but rare in adult tissues. They are the only form of cell found to survive in "necrotic lesions" after radio and chemotherapy of adenocarcinoma in human lungs. In other words, its behavior is consistent with what is expected for the human stem cells of organogenesis and carcinogenesis. Because these metakaryotic cells were not found in the literature, had both a bizarre form and division process, and displayed asymmetric nuclear fission, a shibboleth of stem cells, my research immediately turned to their nuclear organization. I focused particularly on differences in nuclear organization between eukaryotic and metakaryotic cells, which would lead to an understanding of the differences in cell division, gene expression, and other cellular processes. This thinking led to my central thesis question: how are chromosomal elements arranged in metakaryotic nuclei? The following background is a short summary of basic nuclear and DNA structures that are applicable to this thesis, followed by a review of nuclear processes and nuclear organization in the eukaryotic cell, and Dr. Gostjeva's discoveries of, and about, metakaryotic cells.

## 2. BACKGROUND

Given what we know about human gene expression, for example that the molecules in cell nuclei have diffusion limited movements and that sequence dependent cis-elements regulate much of transcription, it seems necessary that the control of gene expression would require some structural organization of the DNA in the nucleus. Indeed, if we pictured ourselves standing in the middle of a nucleus and looked up at the nuclear envelope, we could imagine that the points of DNA attachment to the nuclear matrix would look like the stars in the sky at night, and make their own patterns, or constellations, that would be consistent in all nuclei. "A place for everything and everything in its place." It would follow then, that changing this structure would result in gene expression changes that would define different cell states or cell types, like the changes that occur during differentiation. Therefore, understanding the nuclear organization of the genome appears to be required to fully understand gene expression and all processes that are defined by gene expression. I begin with a review of the main elements of chromatin organization in eukaryotic mitotic cells that preceded the discoveries about metakaryotic cells.

### 2.1 Eukaryotic Mitotic Human Cells: Basic DNA Organization and Nuclear Structures

#### 2.1.1 Chromosomes

The small-scale structure of DNA is commonly known. Double stranded DNA in organisms forms an A, B, or Z-DNA structure, with B-DNA being the most common structure in

somatic cells (Leslie et al., 1980). The B-DNA chain is a right-handed spiral, 22 to 26 Ångströms (Å) wide with 3.3 Å between each DNA base along the backbone, and 10 bases per 360 turn of the helix. As the DNA strands wind around each other, they leave gaps, or grooves, between each set of phosphate backbones. The major groove is 22 Å wide and the other, the minor groove, is 12 Å wide. Because the major groove is wider, the bases are more accessible, and most DNA binding proteins usually make contact in the major groove (Pabo and Sauer, 1984).

Approximately 200 base pairs of double stranded DNA constitutes a nucleosome repeat unit, where 146 base pairs are wound around a nucleosome protein core, and the other 50 base pairs is “linker DNA” which separates the nucleosome core particles. Nucleosomes consist of two pairs of four histone proteins (H2A, H2B, H3 and H4), called the histone octamer, arranged into two H3-H4 dimers and two H2A-H2B dimers. The structure of DNA wound around nucleosomes has been observed at the molecular level by electron microscopy, and resembles “beads on a string.” Intermediate DNA structures between the nucleosome and the chromosome are less certain.

Electron microscopy analysis of nuclei lysed under specific conditions showed a 30 nm fiber. Various nucleosome-coiling models have been suggested for this fiber, none experimentally proven, but the solenoid model is the most accepted. In the 1960s, experiments in which metaphase chromosomes were treated with 2M NaCl and spread on carbon coated grids revealed large DNA loops extending from a central structure, the chromosome scaffold. The loops varied widely around a mean length of 70µm, or 200 kbp (Paulson and Laemmli, 1977). Some preparations gave rosette structures instead of long loops, and radial loops of 50-100 kbp of DNA attached to the chromosomal protein scaffold have been observed under non-physiological conditions, so it remains to be discovered if the loops are attached to the structure in a “rosette” or “radial” structure, and if there is any further condensation of the loops themselves.

The chromosome scaffold itself has a helical structure that has been observed by numerous scientists, including Dr. Gostjeva and myself. The condensation patterns during prophase and metaphase we observe are explained differently in different structural theories. Two possible explanations are that the scaffold itself may be coiling tighter or that the DNA loop structures are being packed closer together on the scaffold. Figure 1 shows the various structures of DNA and chromosomes, both known and theorized.

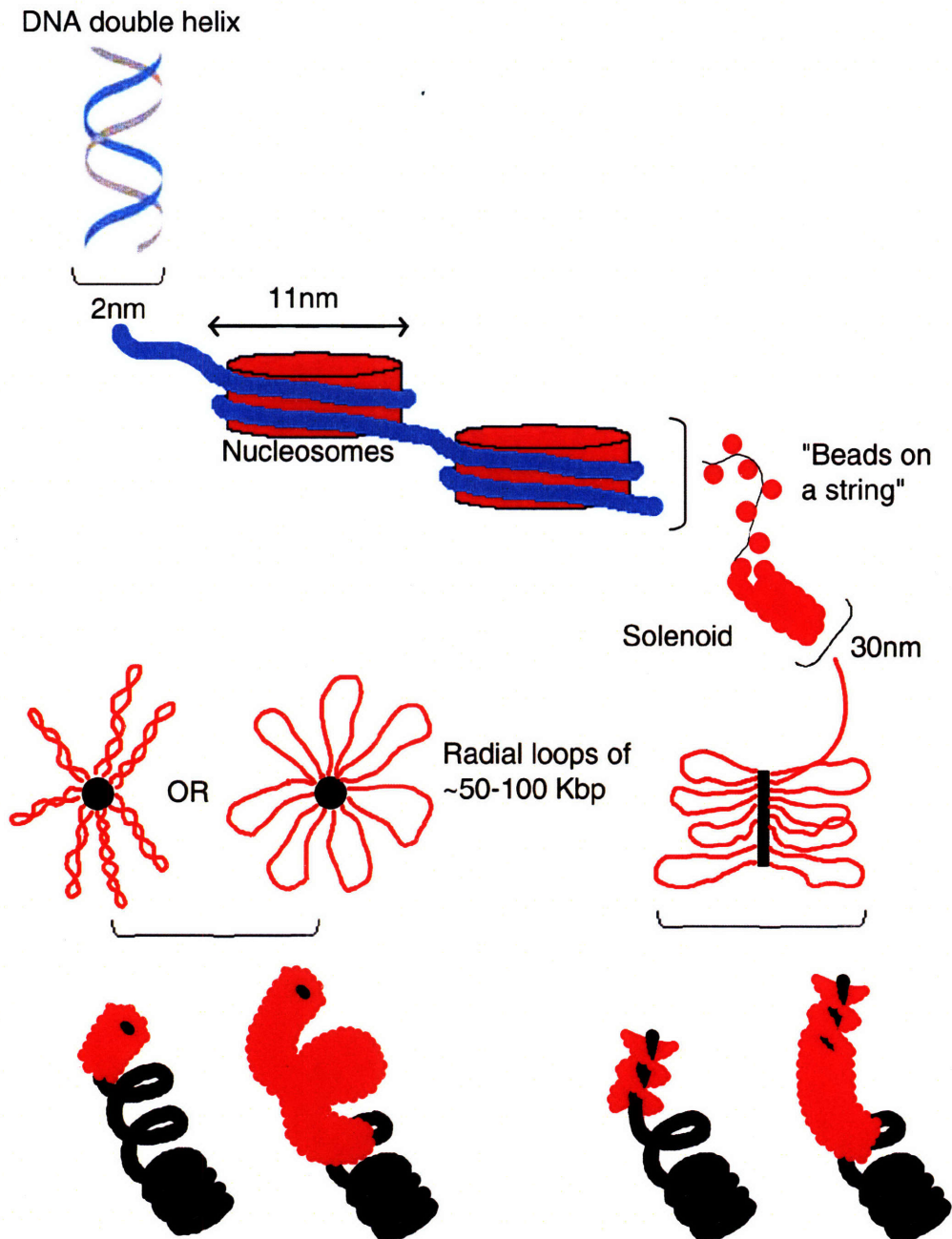


Figure 1. Theories of DNA and chromosome structures. Double stranded DNA is shown in blue, nucleosomes and the solenoid 30nm fiber are shown in red, and the chromosome scaffold is shown in black. The 30nm fiber is attached to the chromosome scaffold in loops, but whether the attachment points are in a "radial" or "rosette" structure, and how the condensation of the chromosome during mitosis is accomplished is still theoretical.

### 2.1.2 Centromeres

Centromeres are transcriptionally inactive, late-replicating regions of heterochromatic DNA on chromosomes that range from about 1 to 7 million base pairs in humans. Centromeres consist of specific DNA sequences, which are, in higher eukaryotes, typical tandem repetitive sequences, often called "satellite DNA." In humans, the primary centromeric repeat unit is called  $\alpha$ -satellite (or alphoid), which is a tandem 170 base pair repeat sequence. This repeat sequence has a large degree of heterogeneity in human cells, even within a centromere region, including inversions, substitutions, additions, and deletions, which makes each sequence chromosome specific and able to be used for identification through hybridization (Wu and Manuelidis, 1980; Yang et al., 1982; Devilee et al., 1986; Jabs and Perisco 1987).

The centromere repeat sequences bind specific proteins called cen-proteins (CENPs). Centromeric DNA is normally condensed into heterochromatin, in which histone H3 is replaced by CENP-A. This replacement is necessary for the proteins that bind sister chromatids to each other and for assembly of the kinetochore on the centromere. Sister chromatids join together at the centromeric regions during the prophase and metaphase stages of mitosis and meiosis. Kinetochore proteins bind to the centromeres, which form an anchor point for the spindle formation required for the pull of chromosomes toward the centrioles during the anaphase and telophase stages of division. The exact roles of CENP-B are still being investigated, but it is necessary for recruitment of other cen-proteins, including CENP-A (Ohzeki et al., 2002), and may repress centromere formation at other sites in the genome (Okada et al., 2007).

### 2.1.3 Telomeres

Telomeres are ribonucleoprotein complexes located at the ends of chromosomes, composed of an RNA primer sequence, several hundred thousand base pairs of DNA repeat sequence, and several proteins. They compensate for the incomplete semi-conservative replication of DNA molecules and protect chromosomal ends from end joining or recombination by distinguishing them from double strand breaks (Lundblad 2000; Ferreira et al., 2004; Nugent and Lundblad 1998).

Telomeres are extended by telomerases, reverse transcriptase enzymes known as TERTs (Telomerase Reverse Transcriptases). However, TERT expression is repressed in many types of human cells, so telomeres shorten with each successive division, although in embryonic stem cells grown in culture, which require extensive divisions, TERT is expressed and telomere length is maintained. Telomere shortening has been linked to senescence and aging, and telomerase has been shown to be activated in some cancer cells.

Telomere length is generally several kilobases in humans, containing the repeat sequence TTAGGG. In human cells, telomeres have long single stranded overhangs of approximately 300 base pairs (Wright et al., 1997) that form G-quadruplex structures (Figure 2) in sodium and potassium solutions (Makita et al., 2005). Sets of four guanine bases are held in plane and then stacked on top of each other with either a sodium or potassium ion between the

planar quadruplexes (Burge et al., 2006; Parkinson et al., 2002). These structures can form from G clusters within the same strand, or have been shown to form from four or more different strands.

In addition to these stacked structures, telomeres also form loop structures called telomere loops, or T-loops. Single-stranded DNA is curled around in a circle and stabilized by telomere-binding proteins (Griffith et al., 1999). At the very end of the T-loop, the single-stranded telomere DNA is held onto a region of double-stranded DNA. This triple-stranded structure is called a displacement loop or D-loop (Burge et al., 2006).

Multiple proteins binding single- and double-stranded telomere DNA have been identified. TRF1 and TRF2 bind double stranded telomeric repeats in humans (Court et al., 2005) and are involved in T-loop structures, along with five other proteins collectively referred to as the shelterin complex (de Lange et al., 2005). Telomere end-binding proteins (TEBPs) bind to the G-rich overhang, and TEBP $\alpha$  and TEBP $\beta$  have been shown to mediate the formation of the G-tetraplex structure in vivo (Paeschke et al., 2005).



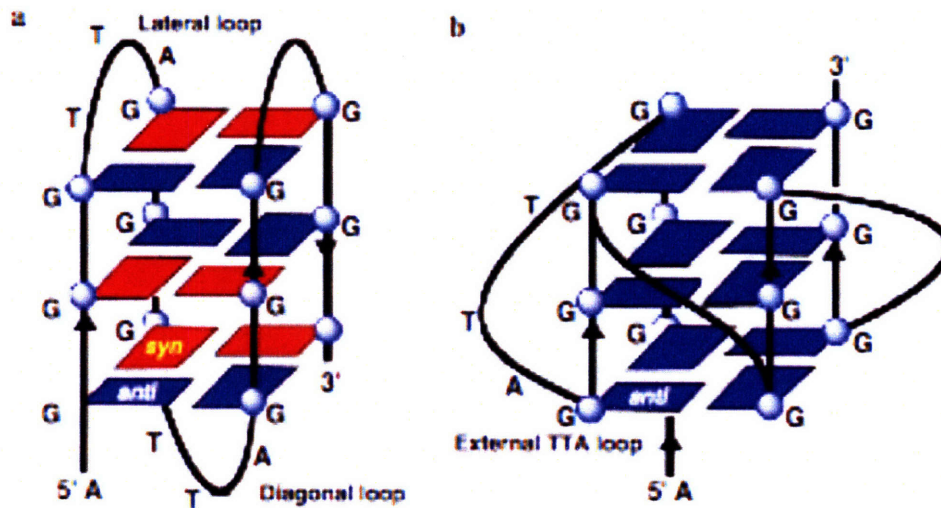


Figure 2: G-quadruplex structures of the human telomere repeat sequence. Blue and red boxes represent the anti and syn confirmations of guanine bases, respectively. a) The Na<sup>+</sup> stabilized solution structure with on diagonal and two lateral TTA sequence connectors. b) The K<sup>+</sup> stabilized crystal structure, with external TTA loops on the sides of the GGG columns. Reproduced with permission from Xu et al., 2006.

## 2.2 Nuclear Organization of Eukaryotic Cells

More than 100 years ago, Rabl and Boveri proposed that the nuclei of eukaryotic cells are highly organized, with each chromosome occupying a specific locations, called a chromosomal territory (CT). Until recently, this has been difficult to test because of the restrictions of microscopy and hybridization techniques. However, in the past 30 years, with advances in technology, we have had major advances in the understanding of nuclear organization.

### 2.2.1 Nuclear Organization of Eukaryotic Cells in Mammals

#### 2.2.1.1 Interphase

In 1982, the Cremer brothers from Munich, Germany, discovered that irradiating specific areas of interphase hamster nuclei damaged discrete chromosomal regions, suggesting that interphase chromosomes occupy specific nuclear positions (Cremer et al., 1982). Several groups used in situ hybridization probes for specific chromosomes and confirmed that each chromosome occupies a specific territory in the nucleus, which does not overlap with other territories (Borden and Manuelidis, 1988; Cremer et al., 1988). Gene dense, early-replicating CTs tend to cluster at the nuclear interior and gene poor, late-replicating territories at the nuclear periphery or the nucleoli (Croft et al., 1999; Boyle et al., 2001). Chromosome territories are separated by interchromosomal spaces with no DNA, theoretically where transcription machinery is found (Zirbel et al., 1993). Figure 3 shows a model of the nucleus incorporating chromosomal territories.

There have been several reports that the localization of chromosome regions is dependent on cell type and/or gene expression, leading to the conclusion that each cell type may have a unique distribution. Human cell types with flat/ellipsoid nuclei (amniocytes and fibroblasts) and spherical nuclei (lymphocytes, keratinocytes, colon and cervix epithelial cells) have different distributions of chromosome 18 (Cremer et al., 2001; Cremer et al., 2003). The positioning of genes within a CT is also regulated, with inactive genes generally located in the territory interior and active genes located on the periphery of the territory, or in some cases, looping out into the interchromatin space (Cremer et al., 2001; Vopli et al., 2000). Active genes are also occasionally seen inside the CT, but it is proposed that transcription machinery can access these areas by infoldings of the CT, or small channels through it like a sponge (Cremer et al., 2006).

The movements of chromosomes in interphase are constrained (Gasser, 2002; Taddei and Gasser, 2004). Chromosomal loci both demonstrate small movements of <0.2 microns, generally thought to be random walk, and larger movements of >0.5 microns, many of which are seen concurrent with changes in cell stage or transcriptional activity. For example, in quiescent human fibroblasts, chromosome 18 repositions itself after exiting the cell cycle into G<sub>0</sub>, and returns to its original position following cell cycle re-entry (Bridger et al., 2000). Additionally, changes in the nuclear positioning of chromosomes 12 and 16 have been observed during human adipocyte differentiation (Kuroda et al., 2004). Movement of

individual genes or chromosomal regions has also been seen. The major histocompatibility complex locus extends away from its chromosome territory when it is being actively transcribed (Volpi et al., 2000), as does the HoxB locus (Chambeyron and Bickmore, 2004).

Human centromeres are located in their respective CT, and therefore are near the nuclear envelope or interior depending on the gene density of their chromosome (Carvalho et al., 2001; Weierich et al., 2003; Gilchrist et al., 2004). Centromeres in lymphocyte nuclei tend to localize to the nuclear periphery and around the nucleoli, except for the centromere of the inactive X chromosome in females, which is found with equal probability in the nuclear interior and periphery (Weierich et al., 2003). Changes in centromere positioning in relation to cell cycle, differentiation or physiological state have been reported (reviewed by Gilchrist et al., 2004), and specific clustering of centromeres during lymphoid and myeloid differentiation (Beil et al., 2002; Alcobia et al., 2003). Wiblin (2005) reports that some chromosomal regions involved in pluripotency have different positioning in human embryonic stem cell lines relative to differentiated cells and have fewer centromeres located at the nuclear periphery.

Three-dimensional analysis indicates that telomeres are located close to the nuclear envelope in some eukaryotes, including *Drosophila* (Mathog et al., 1984) and plants (Rawlins and Shaw, 1990). Human telomeres were reported attached to the nuclear matrix in all phases of the cell cycle (de Lange et al., 1992), but using FISH in human fibroblasts, telomere signals appear to be distributed randomly throughout the nucleus in interphase, so they are not always confined to the nuclear envelope (Nagele et al., 2001). In human cultured lymphocytes, the telomeres of chromosomes were found on the opposite side of chromosome territories from the centromeres (Amrichova et al., 2003), which agrees with the fact that most telomere signals are found in the nuclear interior (Weierich et al., 2003; Amrichova et al., 2003), since most centromeres are found at the nuclear periphery. The same study found that in mouse lymphocytes, most telomere signals are found at the nuclear periphery (Amrichova et al., 2003), likely partly due to the fact that mouse chromosomes are telocentric.

Telomeres are very often found associated in human interphase cells (Henderson et al., 1996; Nagele et al., 2001; Weierich et al., 2003; Amrichova et al., 2003). Most studies concentrated on staining intensity to study telomere lengths and found telomeric associations by chance. For example, the integrated optical density (IOD) of telomere FISH signals was observed in human cultured fibroblasts in G1/G0 quiescence. The fluorescent intensities were varied, but fell into three obvious groups, where the mean of the second and third groups were multiples of the first, suggesting that telomeres were associating, or fusing, during interphase into either dimers or trimers (Nagele et al., 2001). Studies on telomere staining in interphase cells rarely include counts of telomeric regions per cell, so I determined the number of staining regions either from photographs of staining or from other data in the papers. The number varied widely, from 12 to 91 telomeric staining regions in human interphase cells (Weierich et al., 2003; Nagele et al., 2001; Henderson et al., 1996). However, these studies were done on a variety of cell types and cell cycle stages, including quiescent cells. Interestingly, when looking at a graph of the data from all studies, six distinct peaks are seen at about 12, 25, 38, 51, 78, and 91 telomeric staining regions per cell, possibly indicating the telomeric stages of association in human interphase cells. It is unknown whether these telomeric interactions are

the result of inter- or intra-chromosomal associations. In human cultured lymphocytes, the telomeres of chromosome 19 were very frequently associated with each other, possibly forming a loop-like structure (Amrichova et al., 2003). However, in human cultured fibroblasts, the telomere on the short arm of chromosome 14 was always found associated with another telomere that was not on chromosome 14 (Henderson et al., 1996). A link has also been found between immortal cells and telomere associations, as they are found frequently in tumors and immortal cell lines (de Lange et al., 1994). It was originally thought that these telomere associations were the result of telomere shortening, however there has been no link found between telomere shortening and increased telomere associations (Nagele et al., 2001). In fact, telomere associations have been found in Chinese hamster embryonic cells that have normal telomere lengths (Slijepcevic et al., 2000).

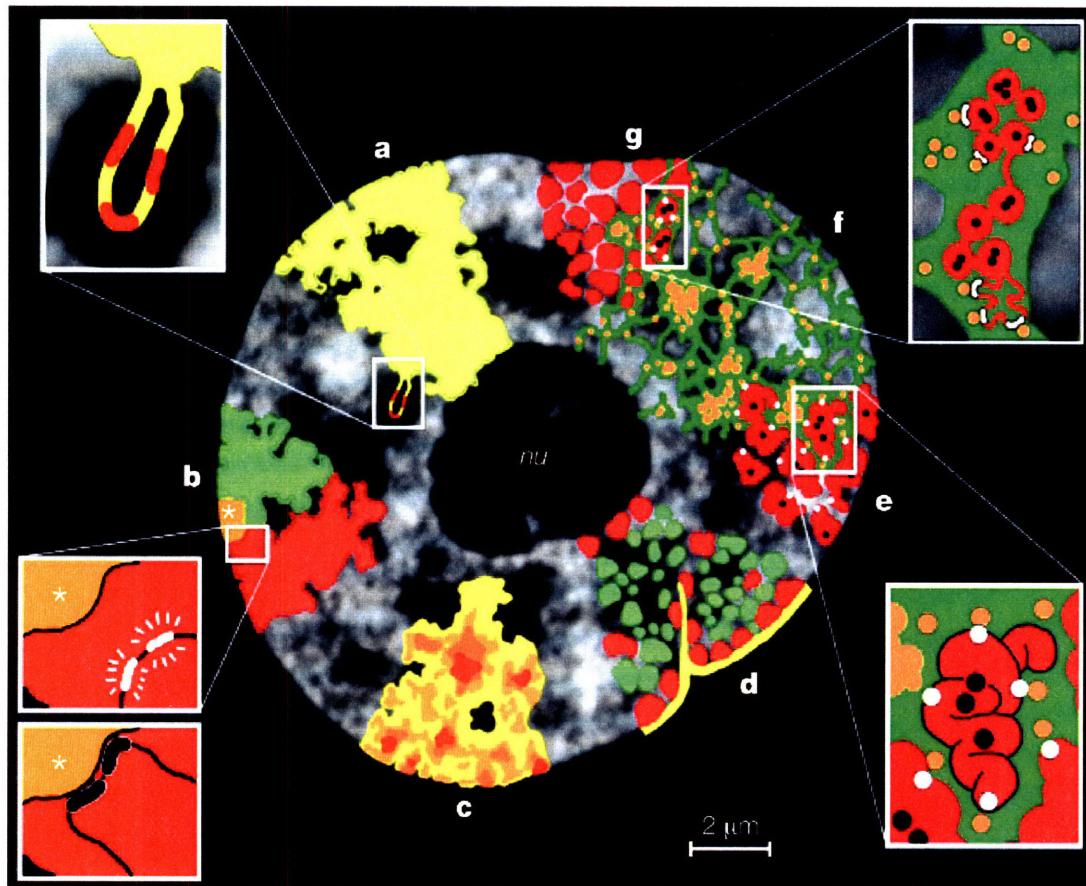


Figure 3: Model of interphase nuclear architecture. This model is drawn roughly to scale over a photo of a HeLa cell nucleus. a) Chromosome territory with inset of active genes looping out into the interchromosomal space. b) The short (green) and long (red) arms of a chromosome occupy different territories, and genes can be actively transcribed or silenced based on their distance from centromeric heterochromatin (yellow with asterisk). c) CTs have variable chromatin density (red = high density, yellow = low density). Low-density chromatin is generally located near the interchromatin space, whereas high-density chromatin is located in the chromosome territory interior. d) Early-replicating domains (green) tend to be in the nuclear interior, and late-replicating domains (red) tend to be associated with the nuclear envelope along the nuclear periphery and near the nucleolus. e), f), and g) Active genes are located along the periphery of higher-order chromatin fibers, and inactive genes are located in the interior. The interchromatin compartments (green) contain complexes and larger aggregates (orange) of proteins for transcription, splicing, repair, and replication. Reproduced with permission from Cremer et al., 2001.

### 2.2.1.2 Mitosis

In eukaryotic cells, the cell cycle consists of four phases: G1, S, and G2 (collectively referred to as interphase) and M. During G1, the biosynthetic activities of the cell, such as transcription and translation, are at a high rate. The cell synthesizes the proteins required for S phase, mostly those involved in replication. The duration of G1 is highly variable. During S phase, DNA replication takes place, and the amount of DNA in the cell is doubled. All DNA sequences have specific replication timing in S phase that is conserved from cell cycle to cell cycle. Heterochromatic regions, including centromeres, are late replicating, but telomeres replicate at various times, suggesting they are most likely replicated with neighboring sequences (Ten Hagen et al., 1990). In humans, S phase takes about 8 hours, and the rates of transcription and translation are at a lower rate during this time. During G2, the rate of transcription and translation resume their higher rate and the cell synthesizes the microtubules required for mitosis and cytokinesis. M phase is when the processes of mitosis and cytokinesis take place. Mitosis is further broken down into prophase, metaphase, anaphase, and telophase. In prophase, the nuclear envelope dissolves and the genome condenses into distinct chromosomes. In metaphase, fully condensed chromosomes are organized into the metaphase plate, or “halo” of chromosomes by the microtubules. In anaphase, the microtubules separate the sister chromatids by their centromeres to segregate the two genome copies to the spindle poles. In telophase, cytokinesis, or cleavage of the cytoplasm takes place between the to form two daughter cells. Cells that have temporarily or reversibly stopped dividing are said to have entered a state of quiescence called G0 phase.

Developments in microscopy and molecular labeling methods now allow the position of chromosomal domains to be followed through time in living cells. When specific CTs are followed through the cell cycle, it has been found that the organization of chromosomes is inherited from mother to daughter. During the progression through mitosis, the metaphase plate organization in the mother cell results in similar relative organization of chromosomal neighborhoods in the two daughter cells after division. The global organization is lost and re-established during early G1, but then there are no large-scale changes in the global organization of chromosomal territories during the rest of metaphase (Essers et al., 2005; Parada et al., 2003; Gerlich et al., 2003; Gerlich and Ellenberg, 2003).

### 2.2.1.3 Meiosis and Gametogenesis

Meiosis can be separated into the same stages as mitosis: prophase, metaphase, anaphase, and telophase. In mitosis, these processes are repeated to achieve a daughter cell with half the original amount of DNA, so the stages are referred to as prophase I and II, metaphase I and II, etc. Prophase I is further broken down into leptotene, zygotene, pachytene, diplotene, and diakinesis. During leptotene (and the pre-leptotene stage), chromosomes condense into separate individuals with their sister chromatids tightly bound together. In zygotene, homologous chromosomes become paired, or associated with each other, through the synaptonemal complex (SC) to form tetrads (four sister chromatids). During pachytene, non-sister chromatid crossovers occur between homologous chromosomes and form chiasmata, but the SC still tightly binds the chromosomes. The SC degrades in diplotene, and the

homologous chromosomes separate slightly, but are still bound at the chiasmata, which are observable. The last stage is diakinesis, in which the chromosomes condense further and all four tetrads are visible. The nucleoli and the nuclear membrane disintegrate and the spindle begins to form for organization and separation of chromosomes.

Telomeres, and to a lesser degree centromeres, are considered key structures in the pairing of homologs during meiosis, as their movements precede the pairing. This has been shown in human and mouse spermatogonia using FISH probes for telomeres, centromeres, and specific loci (Scherthan et al., 1996). In humans and mice, telomeres are randomly distributed during mid-preleptotene, then move to the nuclear envelope during late-preleptotene and move along the nuclear envelope to cluster together during zygotene, forming a chromosomal “bouquet” structure. Telomeres redistribute along the nuclear envelope during pachytene. In both humans and mice, centromeres are moved to the nuclear periphery during mid-preleptotene. In mice, they migrate around the nuclear envelope during late-preleptotene, then cluster during zygotene, and migrate back around to distribute along the nuclear envelope by the pachytene stage. Interestingly, in humans the centromeres are moved into the nuclear interior in clusters during late-preleptotene and stay there through the end of prophase. A comparison of mouse and human centromere and telomere movements in meiosis is shown in Figure 4. Homologous chromosome pairing takes place during the bouquet stage (leptotene and zygotene), and all homologs are paired by the pachytene stage. The clustering of telomeres is important for pairing by bringing homologs in close proximity, but it is not necessary for pairing in all organisms (McKee 2004; Ding et al 2004).

The 3-dimensional nuclear organization of mature human sperm has been determined using various concentrations of heparin to gradually increase the decondensation of sperm cells and observe the locations and interactions of centromeres, telomeres, and chromosome arms using FISH (Zalensky et al., 1993; Zalensky et al., 1995; Zalensky et al., 1997; Zalenskaya and Zalensky, 2004; Solov'eva et al., 2004; Mudrak et al., 2005). Centromeres interact non-homologously to form a compact chromocenter in the middle of the nucleus. Upon minimal nuclear swelling with heparin, one or occasionally two large fluorescent centromere signals were visible. When the concentrations of heparin were increased, dimers and dense linear arrays of centromere signals were seen (Zalensky et al., 1993; Zalensky et al., 1995). In contrast, belts of telomeres were seen around the nuclear periphery in minimally decondensed nuclei (Zalensky et al., 1995; Zalensky et al., 1997), but approximately one quarter the expected number of signals in haploid cells were seen, about 12. When further decondensed, the number of telomeric signals increased to half the number expected, or 23, which is the number of chromosomes in the sperm haploid genome (Figure 5a). Telomere dimers, tetramers, and semicircular arrays also became visible (Figure 6). Only when the nucleus was further decondensed did 46 telomeric signals (twice the number of chromosomes) become visible (Figure 5b). Similar results were observed in mouse, rat, bull, stallion, and boar sperm with the exception that mouse and rat telomeric signals started clustered, similar to human sperm centromeric signals. Based on these results, it was concluded that the telomere dimer was an organizational feature of mammalian sperm cells. Further research demonstrated that the telomere dimers were intrachromosomal, and the chromosomes of human sperm all form hairpin loops with their centromeres pointing in, their telomere dimers pointing out, and their p and q arms overlapping or entwined (Solov'eva et al., 2004; Mudrak et al., 2005).

The movements of centromeres and telomeres during spermiogenesis have also been observed in rats using FISH, and it was shown that the number of centromeres and telomeres decreased as spermiogenesis progressed due to dimerization and clustering (Meyer-Ficca et al., 1998). Centromeric dimers were seen first in stage 6, formed semicircles in stage 9, and had formed one to four clusters per nucleus by stage 10 or 11. Telomeric dimers were seen starting in stage 9, but most were seen in stage 10 through 12, and about 17 telomere signals were seen on average in mature rat sperm.

### 2.2.2 Nuclear Organization in Other Species

During interphase in yeast, centromeres are clustered close to the spindle pole body and telomeres are clustered at the nuclear periphery. Interestingly, in both fission and budding yeast, the number of telomere signals observed with FISH corresponds to either half or one quarter the number expected (Funabiki et al., 1993; Gotta et al., 1996; Laroche et al., 1998), which implies telomeres are associating into dimers and tetramers, similar to mammalian sperm. [Telomere clusters at the nuclear periphery co-localize with Rap1, Sir3p, and Sir4p proteins in budding yeast, mediated by the yeast Ku protein. The interaction of these proteins is necessary for telomere silencing which shows a direct link between gene expression and nuclear architecture (Gotta et al., 1996; Laroche et al., 1998).]

In budding yeast, there is evidence for and against pairing of homologous chromosomes in somatic cells, but premeiotic pairing has been reported in >95% of cells in fission yeast (McKee, 2004). In fission yeast, meiosis involves nuclear oscillation in order to shuffle homologs close together so centromeres can pair without telomere clustering (Ding et al., 2004). During mitosis in fission yeast, centromere and telomere clusters are dissociated and arranged linearly between the spindle pole bodies, then migrate with them during anaphase and reestablish their clusters during telophase (Funabiki et al., 1993).

In both *Drosophila* polytene chromosomes and *Drosophila* embryonic cells, centromeres are clustered near the top of the nucleus and telomeres are at the bottom, what is referred to as a Rabl configuration (Mathog et al., 1984; Hiraoka et al., 1990). During the transition from prophase to metaphase, this orientation is conserved, and the telomeres of chromosomes are frequently found to be associated in dimers. Polytene chromosomes were also observed to occupy discrete territories in the nucleus. Homolog pairing in *Drosophila* somatic and germ line cells takes place through most of the cell cycle, probably a dynamic pairing and unpairing process, but that is still a subject of debate. However, 100% of homologs are paired prior to the onset of meiosis, regardless of whether recombination takes place (McKee, 2004).



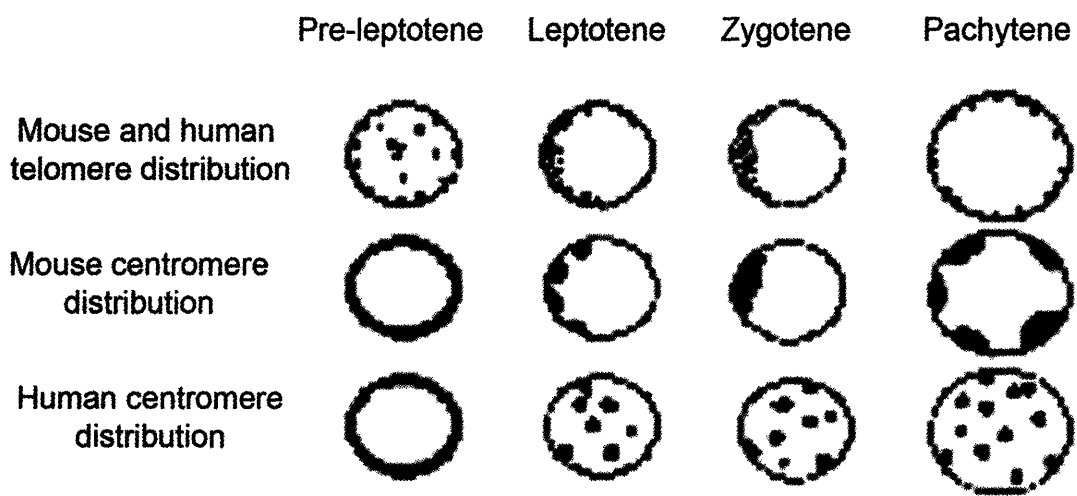


Figure 4: Centromere and telomere organization in mouse and human meiosis. Both mice and humans have the same telomere distribution during the phases of meiosis, but in mice, the centromere clusters stay close to the nuclear envelope after pre-leptotene. In humans, centromere clusters are seen throughout the nucleus after pre-leptotene. Reproduced with permission from Scherthan et al., 1996.

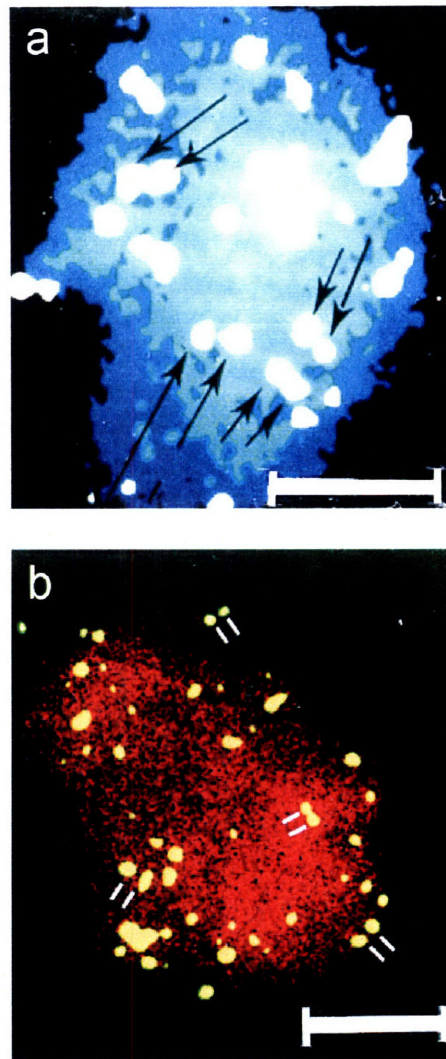


Figure 5: Telomere associations in human sperm cells. Telomeres were stained using a biotinylated  $(TTAGGG)_n$  DNA probe detected by FITC avidin, shown as white in a), yellow in b), and total nuclear DNA was counterstained with propidium iodide, shown as blue in a), red in b). Human sperm cells were swollen with low and medium concentrations of heparin in the presence of 1mM DTT to show the disintegration of telomere associations: a) 0.02 mg/mL b) 0.4 mg/mL. Double lines show examples of telomere dimers and arrows show higher order associations. Bars = 5  $\mu$ m. Reproduced with permission from Zalensky et al., 1997.

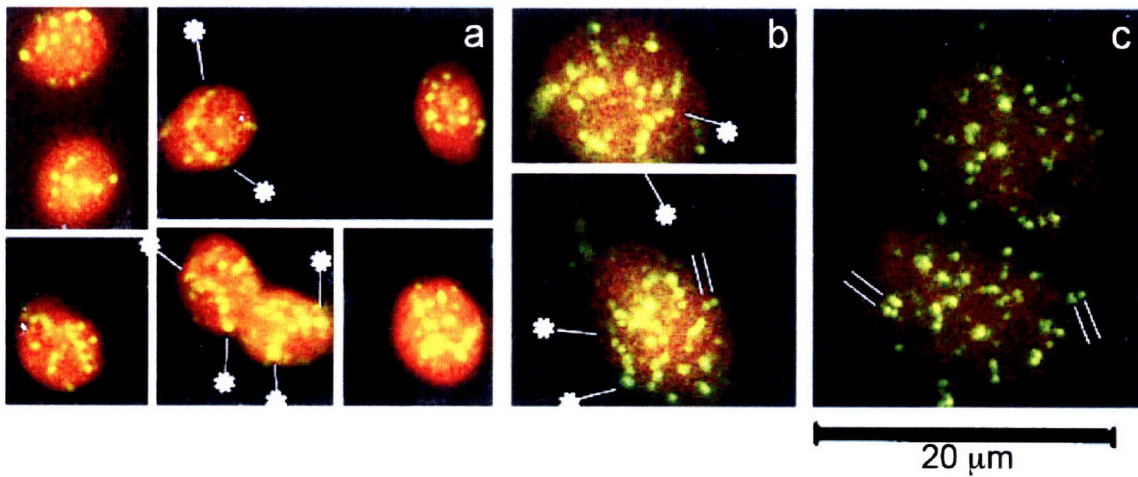


Figure 6: Telomere localization in human sperm cells. Telomeres were stained using a biotinylated  $(TTAGGG)_n$  DNA probe detected by FITC avidin (yellow/green) and total nuclear DNA was counterstained with propidium iodide (red). Human sperm cells were swollen with increasing concentrations of heparin: a) 0.0 mg/mL b) 0.05 mg/mL c) 0.1 mg/mL. All panels are the same magnification. Double lines show examples of telomere dimers and asterisks show the beginnings and end of telomere belts or semicircles. Reproduced with permission from Zalensky et al., 1997.

## 2.3 Metakaryotic Cells

In September 2003, Dr. Elena Gostjeva reported that in human fetal tissue, normal somatic tissue, adenomas, and adenocarcinomas and their derived metastases, cells have several reproducible nuclear shapes: spherical, ovoid, cigar-shaped, bullet-shaped, bean-shaped, sausage-shaped, and bell-shaped nuclei (Gostjeva et al., 2006). The cells with bell-shaped nuclei she dubbed "metakaryotic," since they undergo symmetric and asymmetric division using an amitotic process that is concurrent with DNA synthesis. Dr. Gostjeva uses very specific and careful techniques for observing these cells (which we suppose is one of the reasons their observation has not been recorded before now). She only uses fresh surgical discards that can be fixed within 30 minutes of leaving the body, because within 45 minutes after surgical excision, the bell-shaped forms degenerate into quasi-spherical blobs. About 1mm of tissue is spread carefully in one direction on a slide, being careful not to use too much pressure to destroy the physiological structures. She observes the nuclear structures either using DAPI or the Feulgen reaction to stain DNA. Dr. Gostjeva has found metakaryotic nuclei in all fetal proto-organs, including gut, trachea, brain, spinal cord, and cardiac muscle. Metakaryotic nuclei have also been found in both animals and plants, so these cells appear to be the stem cell lineage in many, if not all, eukaryotes (Figure 7).

### 2.3.1 Basic Structure and Developmental Stages

Metakaryotic nuclei are bell-shaped, with a hollow, open-mouthed nuclear structure that has condensed DNA in two "rings" around the rim. Based on Dr. Gostjeva's analysis of quantitative Feulgen staining (Hardie et al., 2002) and comparison with other nuclei, metakaryotes have the diploid DNA content expected of human non-gamete nuclei, and the two condensed rings around the rim each contain approximately 5% of the DNA in the entire bell.

Metakaryotic cells arise from embryonic stem cells by amitosis 'à ceinture' between the 4th and 7th weeks of life. After their conception, and up to about 12 to 14 weeks, they enter a syncytial phase, where they exist inside syncytia, or structures that resemble myotubes (early muscle fibers). The syncytia are found in clusters in fetal organs, and they autofluoresce, so they are easy to find, but even without visualizing the syncytia, you can see the metakaryotes are in "stripes" (Figure 8). The two daughter cells from the original amitosis will duplicate outwards, with all their daughter bell-shaped nuclei pointing the same direction. The syncytia disappear around 12 to 14 weeks of life and the metakaryotic cells develop balloon-like, autofluorescent projections, which we assume persist through the neonatal and pediatric stages of life until the end of the juvenile period (Figure 9). The hypothesis is that most are terminated by changing into adult mitotic maintenance stem cells, leaving a few as pluripotent regenerative stem cells in adult tissues (Gostjeva and Thilly, 2005). In about one out of every thousand adult colonic crypts, Dr. Gostjeva observed a single, extrasyncytial metakaryotic cell at the base of the crypt, as shown in Figure 10a.

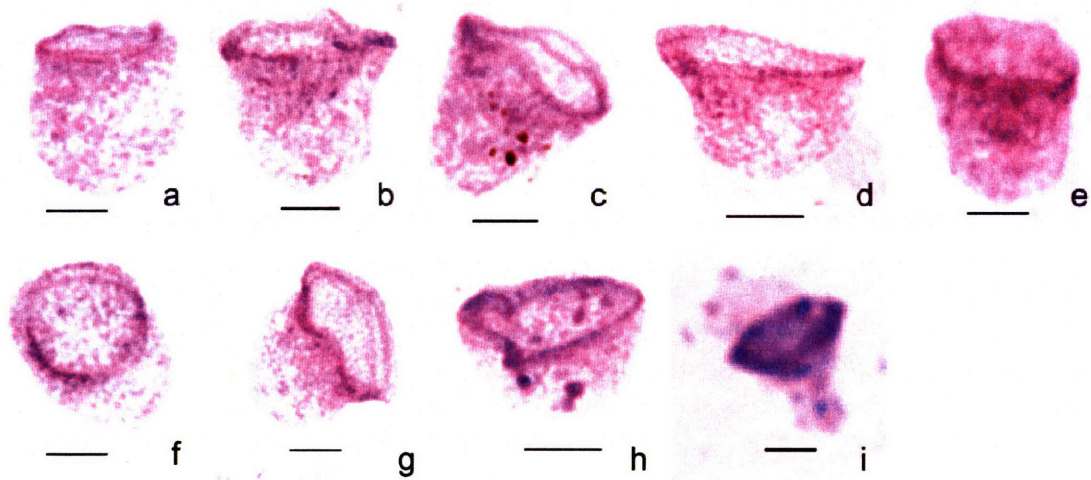


Figure 7: Distribution of bell-shaped nuclei in human fetal proto-organs and other organisms. a-e are metakaryotic nuclei from human fetal tissue found encased in multinuclear tubular syncytia. a) hindgut (7 weeks); b) trachea (10 weeks); c) brain (9 weeks); d) spinal cord (9 – 10 weeks); e) cardiac muscle (10 weeks). f-i are metakaryotic nuclei from various organisms. f) human fetus (8 weeks); g) rat fetus (18 days); h) mouse fetus (16.5 days); i) Arabidopsis embryo (48 hours). Bars = 5  $\mu$ m. Unpublished image used with permission of Dr. Elena Gostjeva. Photomicrographs and histology provided by Dr. Elena Gostjeva.

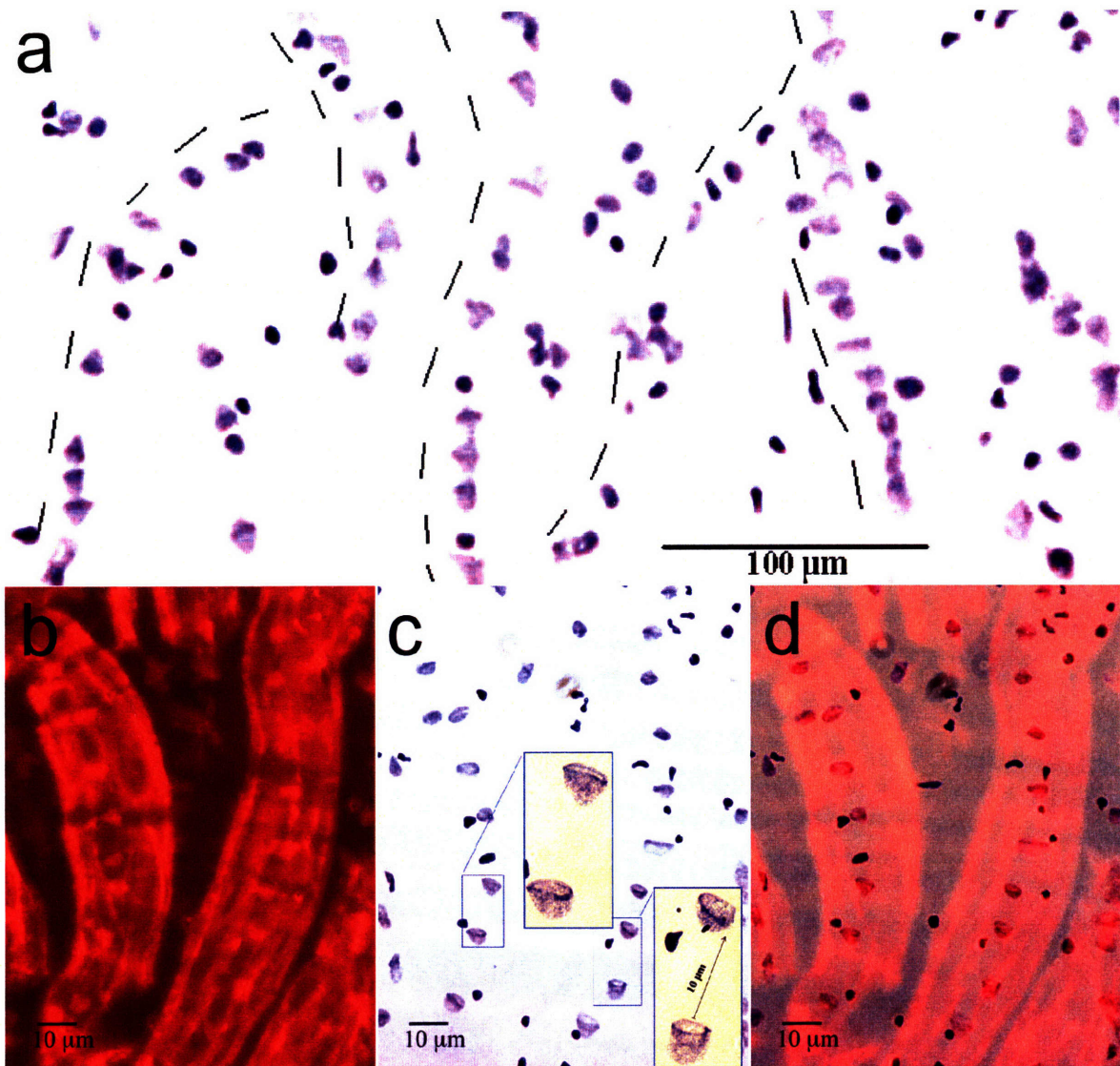


Figure 8: Metakaryotic cells in syncytia from human fetal gut at 5-7 weeks. a) Low magnification of Feulgen stained nuclei. Metakaryotic nuclei are arranged in lines, or “stripes,” (indicated by dashed lines). b) Phase-contrast autofluorescent, c) Feulgen stained, and d) merged image of lines of metakaryotic nuclei incased in autofluorescent syncytia. Reproduced with permission from Gostjeva et al., 2006. Photomicrographs and histology provided by Dr. Elena Gostjeva.

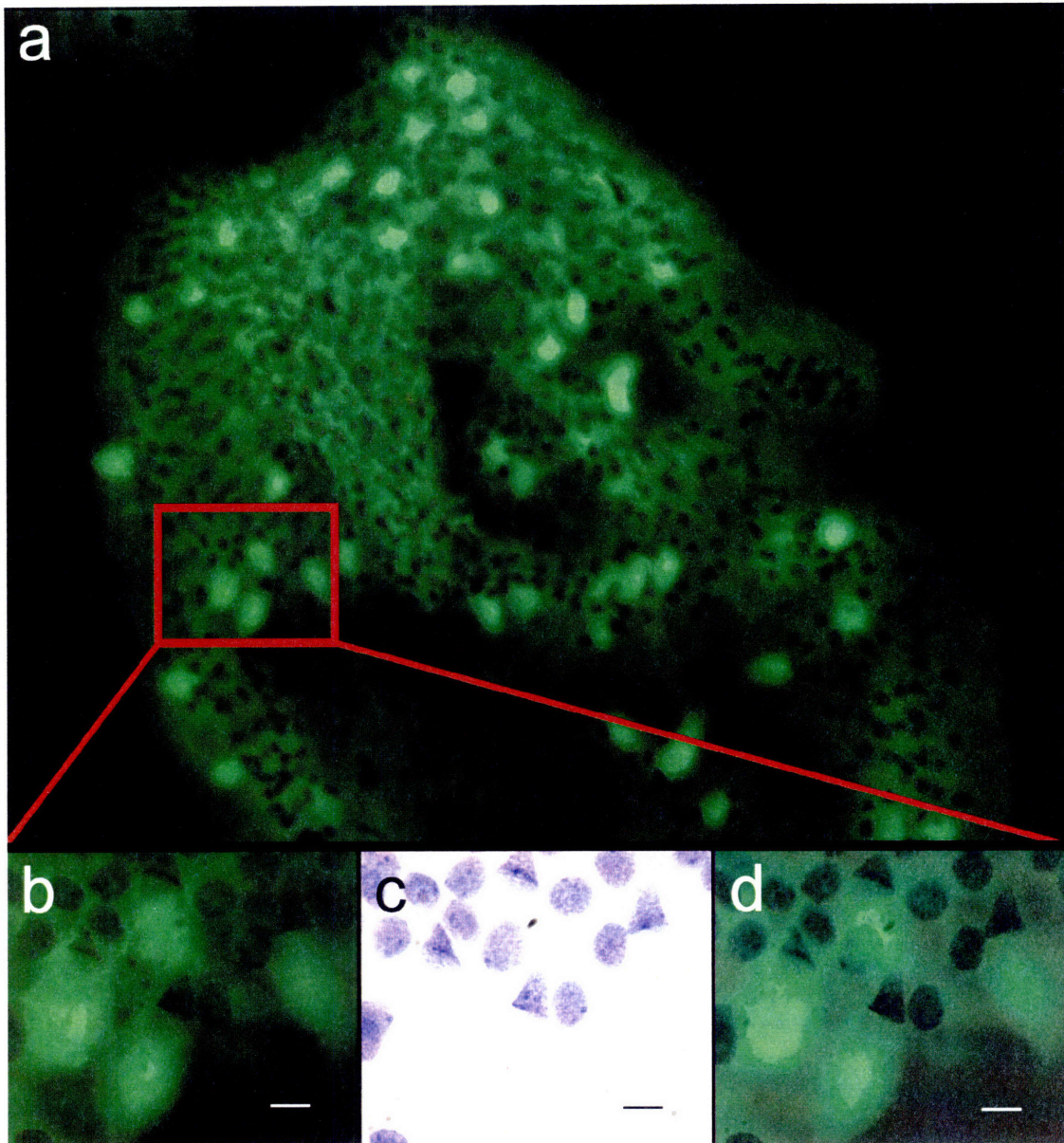


Figure 9: Extracytoplasmic metakaryotic cells from human fetal intestine at 13 weeks. a) Low magnification showing autofluorescent projections from metakaryotic nuclei. b) Phase-contrast autofluorescent, c) brightfield Feulgen stained, and d) merged image of metakaryotic cells with autofluorescent “balloon-like” projections from the mouths of their bell-shaped nuclei. Bars = 10  $\mu\text{m}$ . Unpublished image used with permission of Dr. Elena Gostjeva. Photomicrographs and histology provided by Dr. Elena Gostjeva.

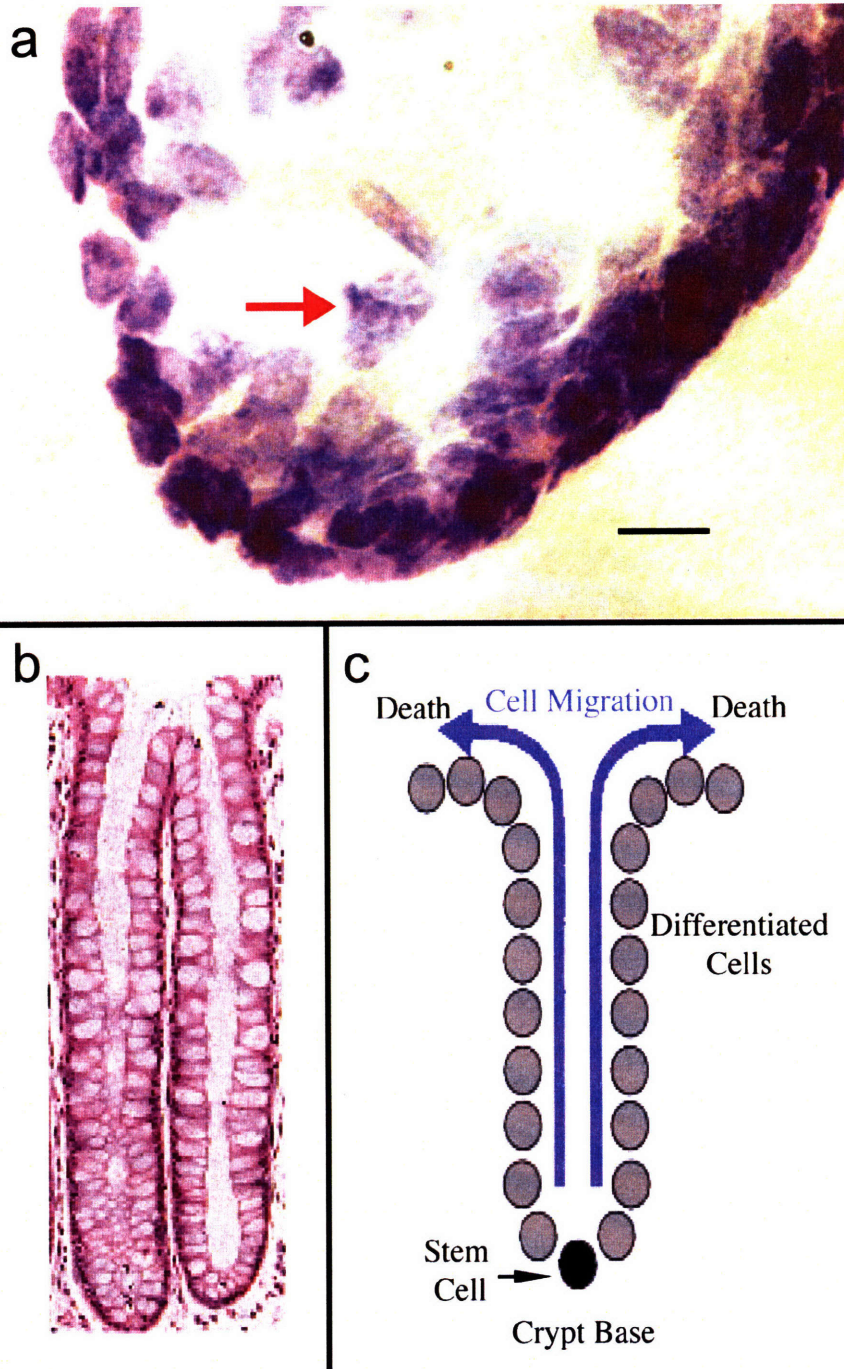


Figure 10: Metakaryotic cells in normal human adult colon tissue. a) Feulgen stained adult colonic crypt showing a single metakaryotic nuclei at the base (Bar = 10  $\mu$ m). b) Feulgen stained adult colonic crypts. c) Cartoon showing cell division and migration in adult colonic crypts. Single stem cells at the base of the colonic crypts divide to form differentiated cells that divide and migrate up the sides and eventually out of the crypts. Reproduced with permission from Gostjeva et al., 2006. Photomicrographs and histology provided by Dr. Elena Gostjeva.



### 2.3.2 Metakaryotes and Carcinogenesis

Dr. Gostjeva observed extrasyncytial metakaryotes frequently in adenomas and adenocarcinomas of the human colon. One, two, or sometimes more metakaryotic cells were found in each crypt, or crypt-like structure, and not always at the bottom. Some metakaryotic cells were found in “ring” structures that contained exactly 8, 16, 32, 64, or 128 cells of a single nuclear morphotype (Gostjeva et al., 2006). No metakaryotes were found undergoing symmetrical or asymmetrical division in adenomas. In contrast, metakaryotes were seen undergoing symmetric and asymmetric division in adenocarcinomas and their derived metastases (Figure 12) (Gostjeva et al., 2006).

### 2.3.3 Amitotic Division of Metakaryotes

Unlike the other nuclear shapes, the bell-shaped nuclei divide by an unconventional amitotic method. Eukaryotic cells synthesize their DNA in S phase, condense it into individual chromosomes with sister chromatids attached to each other, organize the chromosomes into a halo, and pull them apart using microtubules. In other words, eukaryotic nuclei accomplish fission through mitosis. These metakaryotic nuclei do not appear to have any of these steps.

Between the 4th and 7th weeks of life, these cells arise from mitotic embryonic cells, as stated above. They divide by a form of “à ceinture” amitosis, similar to a form of amitosis seen in protozoans (Orias et al., 1991; Prescott et al., 1994; Cheng and Zou, 2005). During both the syncytial and extrasyncytial phases, metakaryotes divide both symmetrically and asymmetrically. The symmetric divisions take place amitotically in a “cup-from-cup” process. Dr. Gostjeva analyzed the amount of DNA during each step of the separation with Feulgen stain and image processing, and determined that DNA synthesis is actually concurrent with the separation (Figure 11) (E. Gostjeva, personal communication, 2008). Metakaryotic cells divide asymmetrically to produce cells with all other nuclear shapes observed. These other nuclear shapes then divide by conventional mitosis. Here you can see the same “cup-from-cup” nuclear fission process creating another bell-shaped nucleus and a cigar-shaped nucleus. Indeed, Dr. Gostjeva has observed seven different nuclear morphotypes that arise from metakaryotic nuclei, and all of these forms subsequently divide by mitosis (Figure 12).

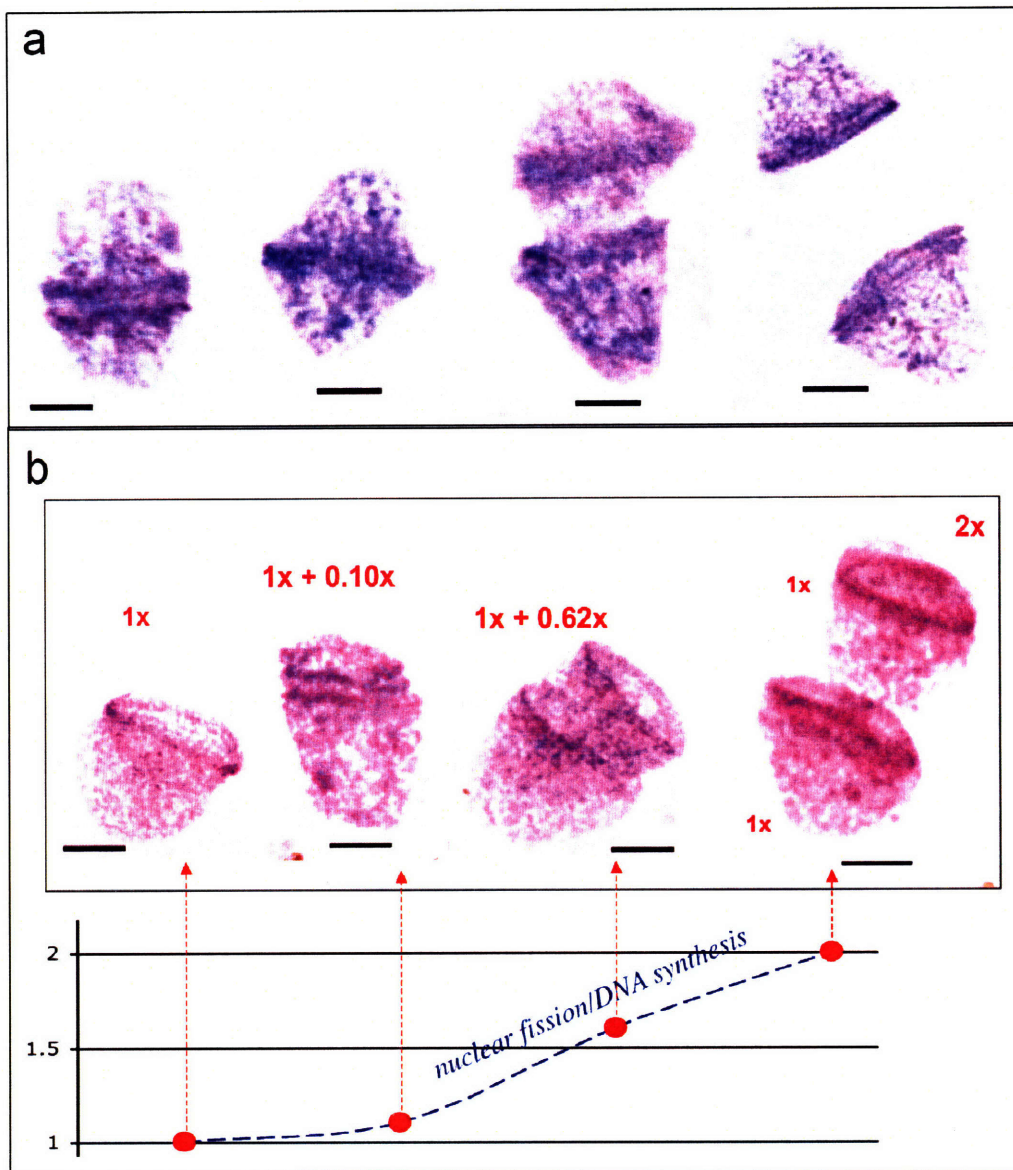


Figure 11: Metakaryotic division processes. a) Feulgen stained metakaryotic nuclei showing amitosis “à ceinture” from left to right. b) Feulgen stained metakaryotic nuclei showing “cup-from-cup” amitosis from left to right concurrent with DNA synthesis. Bars = 5  $\mu\text{m}$ . Reproduced with permission from Gostjeva et al., 2008 (manuscript in preparation). Photomicrographs and histology provided by Dr. Elena Gostjeva.

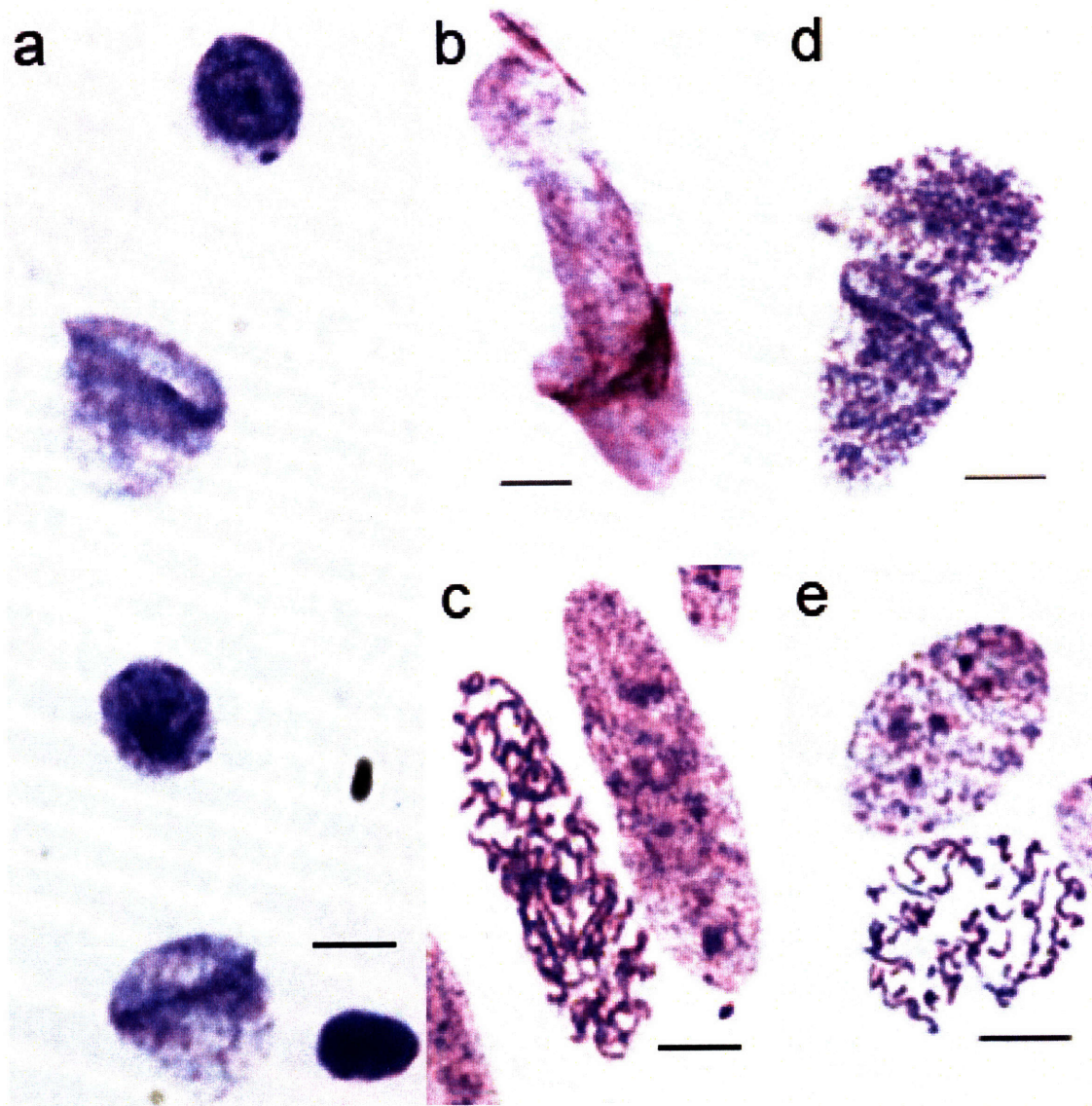


Figure 12: Asymmetric amitotic division of human metakaryotic nuclei and mitotic division of other nuclear morphotypes. Metakaryotic nuclei divide asymmetrically through amitosis to produce all other nuclear morphotypes seen in fetal tissues, which subsequently divide by mitosis. a) Asymmetrically dividing metakaryotic nuclei from fetal gut producing condensed spherical nuclei in syncytia. b) Asymmetrically dividing metakaryotic nucleus in colon adenocarcinoma producing cigar-shaped nucleus. c) Cigar-shaped nuclei in colon adenocarcinoma during interphase and prophase stages. d) Asymmetrically dividing metakaryotic nucleus in fetal gut producing spherical-shaped nucleus. e) Ovoid-shaped nuclei in colon adenocarcinoma during interphase and prophase stages. a) unpublished image used with permission of Dr. Elena Gostjeva. b), c), d) and e) reproduced with permission from Gostjeva et al., 2006. Bars = 5  $\mu$ m. Photomicrographs and histology provided by Dr. Elena Gostjeva.

### 3. MATERIALS AND METHODS

#### 3.1 TK6 Cell Lines

The TK6 B-lymphoblastoid cell line is a diploid human lymphoblastoid cell line heterozygous for thymidine kinase, derived from the cell line WI-L2 (Liber et al., 1982), which was originally derived from a 5 year old male patient with hereditary spherocytosis (Levy et al., 1968, Levy et al., 1971). The TK6 cell line was established after treatment with ICR-191, a frameshift mutagen (Skopek et al., 1978). TK6 cells grow well in suspension and have a relatively stable karyotype in culture.

TK6 cells were grown in antibiotic-free RPMI 1640 medium with L-glutamine (Gibco Labs, Grand Island, NY) and supplemented with 5% horse serum (Sigma). Incubators were kept humidified at 37°C and 5% CO<sub>2</sub> (Oller et al., 1989). Cultures were started in 100mL flasks and transferred to spinner flasks after the first day of growth. Cultures were counted daily and diluted to 4 x 10<sup>5</sup> cells/mL when they reached 1.4 to 1.6x10<sup>6</sup> cells/mL to ensure exponential growth at all times. (between 2 x 10<sup>5</sup> and 1.6 x 10<sup>6</sup> cells/mL). Excess cells were frozen in 10% DMSO supplemented medium and kept at -70°C. Cultures were checked bi-annually for mycoplasma infection and weekly for fungal and bacterial infection, usually on the day of fixation.

#### 3.2 Tissue sources and preparation

Adult normal and tumor tissue were surgical discards from Massachusetts General Hospital, Department of Pathology, including normal adult colon, colon polyps from adenomatous polyposis coli (APC) cases and colon adenocarcinomas. Fetal tissue was obtained from archival slide collections of contributing hospitals, approved by COUHES.

1 cm<sup>2</sup> sheets of colonic mucosa or approximately 1mm thick sections of adenomas or carcinomas were placed in 3x volume fresh 4°C Carnoy's fixative (1:3, glacial acetic acid to methanol) within half an hour of removal (bell-shaped nuclei appear to undergo autolysis by 45 minutes after surgical removal). Fixative was replaced 3 times (at 45 minute intervals), and stored in 70% methanol at -20°C. Samples were rinsed in distilled water and placed in room temperature 45% acetic acid for 15 to 30 minutes to facilitate spreading by maceration.

#### 3.3 Slide preparation

##### 3.3.1 TK6 Cells

Only cultures in log phase growth were used for FISH experiments. (Cultures for fixation were sampled between 10AM and 1PM because they were determined to give the highest mitotic index during this time of day.)

### 3.3.1.2 TK6 Karyotypes

Karyotypes of three separate TK6 cell cultures (TK6-2, TK6-46, TK6-48) were done by Dr. Anne Higgins at Brigham and Women's Hospital to check chromosomal ploidy and irregularities. TK6 cells were dosed with colcemid 1 hour before harvesting. Cells were fixed and spun down. Slides were dropped and stained with Giemsa and examined for distribution of nuclei and to ensure all nuclei were intact.

### 3.3.1.2 TK6 FISH Controls and Optimization Trials

For every fixation, about 12mL of culture was distributed into Eppendorf tubes and spun down at 14,000 rpm in a tabletop centrifuge for 5 minutes. The medium was removed and very fresh (mixed 1 minute before fixation) cold (4°C) Carnoy's fixative (1:3, glacial acetic acid to methanol) was added to approximately  $1 \times 10^6$  cells/mL. The fixations were refrigerated at 4°C and the fixative was changed three times in 1.5-2 hours (first change within 5-10 minutes). Fixations were used immediately for slides after the 1.5-2 hours. Fixative was replaced with 45% acetic acid to a concentration of  $5 \times 10^5$  to  $1 \times 10^6$  cells/ $\mu$ L and vortexed until uniformly resuspended (5-15 minutes depending on the size of the pellet). Cell suspensions were combined and spun down again. Cell concentration was adjusted to about  $5 \times 10^6$  cells/mL and pellet was vortexed back into suspension. Between 1 and 3 drops of suspension were put onto each slide. The suspension was carefully covered with a coverslip and 6 layers of filter paper (S&S). Slides were "squashed" in one direction 3 times with the flat end of tweezers and frozen on dry ice. The coverslip was removed when the slides were completely frozen and slides were dried vertically. Slides were examined for nuclei distribution and to ensure all nuclei were intact.

### 3.3.2 Tissues

Small pieces (0.5mm<sup>2</sup>) of the macerated tissue were transferred to slides with a few microliters of 45% acetic acid and coverslipped. The coverslips were covered with 6 layers of filter paper (S&S) and the tissue was gently spread in one direction with using the flat end of a pair of tweezers. Slides were frozen on dry ice for 5 to 15 minutes, then the coverslips were removed, and the slides were dried at room temperature for about an hour. Slides were examined for nuclei distribution and to ensure all nuclei were intact.

### 3.4 Fluorescence In Situ Hybridization (FISH)

Fluorescence In Situ Hybridization, or FISH, is a process in which fluorescently tagged DNA probes complementary to the sequence you want to observe are bound to the DNA in the sample of interest. The DNA in the sample and the probe DNA are both denatured either together or separately using heat or chemicals (DNA intercalating agents) or both, in this case.

FITC-labeled human pan-centromeric and pan-telomeric probes were bought from Cambio (Cambridge, UK) and their protocols were optimized for use with interphase nuclei and fetal tissue. Probes were prepared from DOP-PCR amplified DNA obtained from flow-sorted

chromosomes. Pan-centromeric probes are alpha-satellite repeat sequences, specific to each chromosome. Pan-telomeric probes are generated using two primers that contain the telomeric repeat sequence TTAGG. FITC-labeled human whole chromosome 6 probes were bought from Vysis (Abbott Park, IL) and their protocol was optimized for use with interphase nuclei and fetal tissue.

#### 3.4.1 Positive TK6 FISH controls

For FISH, slides were dehydrated sequentially in ice cold 70%, 80%, and room temperature 100% ethanol for 2 minutes each and dried completely. Slides were then denatured in 70% formamide/2xSSC at 72°C for 2 minutes and immediately dehydrated again with the same sequence and dried completely. Hybridization mixtures were prepared that contained 7µL hybridization buffer, 2µL sterile water, and 1µL probe. Mixtures were denatured at 72°C for 8 to 12 minutes and immediately added to slides which were then coverslipped, sealed with rubber cement, and put at 37°C in a dark, humidified box overnight.

#### 3.4.2 TK6 and Tissue Whole Chromosome Probe FISH Protocol

Slides were dehydrated in cold 70% ethanol, cold 80% ethanol, and room temperature 100% ethanol for 2 minutes each and dried completely. Slides were denatured in 70% formamide, 2xSSC at 72°C for 50-60 seconds, depending on the extent of acetic acid denaturation. Slides were dehydrated again in cold 70% ethanol, cold 80% ethanol, and room temperature 100% ethanol for 2 minutes each. Hybridization mix included 7 µL hybridization buffer, 1.5 µL sterile H<sub>2</sub>O, and 1.5 µL Whole Chromosome Paint probes (Vysis) with either Spectrum Orange or Spectrum Green fluorescent dye. Hybridization mix was denatured for 5-10 minutes at 72°C and slides were dried completely. Hybridization mix was applied to the slides, coverslipped and sealed with rubber cement. Slides were incubated overnight at 37°C in a humidified box. The next day, slides were washed in 50% formamide, 2xSSC at 42°C twice for 8 minutes each. (Coverslips slid off quickly during the washing process.) Slides were washed with 2xSSC at 37°C for 8 minutes and then washed three times in 1xPBD (0.05% Tween, 4xSSC) at room temperature for 1 minute each. 10 µL DAPI II Antifade, 125ng/mL (Vysis) and coverslips were added. The excess DAPI II Antifade was blotted away and the slides were sealed with rubber cement. Slides were kept in the dark at -20°C when not being imaged.

#### 3.4.3 TK6 and Tissue Centromeric/Telomeric FISH Protocol

Slides were dehydrated in an ethanol series (70%, 90%, and 100%) for 2 minutes each, then air dried, and put in 70% formamide/2xSSC at 70°C for 55 seconds to denature DNA. Slides were immediately put through an ice-cold ethanol series (70%, 90%, 100%) for 2 minutes each to stop denaturation, then air dried. Probe stocks were warmed for 5 minutes at 37°C, mixed, and distributed into Eppendorf tubes. Probe aliquots were denatured with heat (87+/- 2°C for centromere probes, 92+/- 2°C for telomere probes) for 10 minutes, then immediately put on ice for 5 to 10 minutes. 11-12 µL of probe per 22x22mm section was applied to slide and coverslipped. Slides were sealed with parafilm and put in a humidified chamber overnight (16-24 hours). Coverslips were removed in 2xSSC at 37°C for 5 minutes. Slides

were washed twice in 50% formamide/2xSSC at 37°C for 5 minutes each, then twice in 2xSSC at room temperature for 5 minutes each. Before slides were dry, 12-15  $\mu$ L of DAPI/Antifade (Qbiogene) per 22x22mm section was applied to slide. Slides were coverslipped, sealed with rubber cement, and kept in the dark at -20°C when not in use.

### 3.5 Imaging

#### 3.5.1 Microscopy

2-dimensional images were obtained using a KS-400 Image Analysis System from Zeiss (Germany) which includes an Axioplan 2 fluorescent microscope with motorized stage, an AxioCam color CCD camera, and a desktop computer with Zeiss KS-400 software package, developed in part by Dr. Gostjeva in the former Soviet Union (the present Ukraine). Apotome z-stack 3-dimensional images were obtained using an Axioscope System from Zeiss (Germany) which includes an Axioscope fluorescent microscope with motorized stage, an AxioCam black and white CCD camera, and a desktop computer with Zeiss software package.

Slides were observed in phase contrast after drying to ensure good spreading and/or high numbers of mitotic cells. Cell spreads were imaged using a Phase 2 condenser and a regular 40x objective. DAPI and FITC images were obtained using a standard mercury lamp, an 100x oil objective, and DAPI and FITC microscope emission and excitation filters (Zeiss), respectively. The DAPI filter excites at 365 nm and emits at 420 nm (blue) and the FITC filter excites between 450 and 490 nm and emits at 515 nm (green). Images were taken with a 1.4/100x Axioplan oil objective with resolutions of 1030x1300, 2060x2600, or 3090x3900 pixels. When possible, multiple images of one field were taken, changing the focal plane in the z-direction to obtain data through a nuclear cross-section for analysis.

#### 3.5.2 Image analysis

The KS-400 software package (Zeiss) and Adobe Photoshop CS2 version 9.0.2 (Adobe Systems Inc.) were used for all image processing, including making composite images of photos from different filters, adjusting brightness and contrast of pictures, counting signals, etc. For images of one cell with multiple focal planes, each image was separately counted and then overlapped with the others to get a 3-dimensional count of fluorescent signals per nuclei. Fluorescent telomeric and centromeric signals were considered associated (a doublet) and counted as one staining region if the distance between the signals was less than the diameter of the smaller signal, the signals were pointed in the same direction (signals often had “tails”), and were of similar size and fluorescent intensity, the usual method for determining signal associations in this field (Zalensky et al., 1997; Scherthan et al., 1996). All images are on file with the Thilly/Gostjeva Lab at MIT.

## 4. RESULTS

### 4.1 Controls

In order to determine if the FISH probes were binding sufficiently to all targets, and to get eukaryotic centromere and telomere counts to compare to metakaryotic counts, counts were taken of fluorescent signals in positive controls: human lymphoblastoid cells in culture and eukaryotic fetal cells on the same slides as the metakaryotic cells.

#### 4.1.1 Centromere Counts

##### 4.1.1.1 Human Lymphoblastoid Cell Line (TK6)

My first controls were pseudo-diploid TK6 lymphoblastoid cells grown in culture. TK6 cell cultures stayed in log phase growth during times of fixation and had a doubling time that ranged from 13 to 24 hours. Karyotypes of cultures were done by Dr. Anne Higgins at Brigham and Women's Hospital to check chromosomal ploidy and irregularities. Three TK6 cultures were done, including a culture frozen in 1986 (the oldest we found) to get as close as possible to the chromosomal karyotype of the original passage. For cultures TK6-2 and TK6-46, 5 cells were counted and 2 were karyotyped. For culture TK6-48, 4 cells were counted and karyotyped, but chromosome number varied widely so karyotyping was difficult and incomplete. TK6 chromosome number varied from 36 to 47 chromosomes per cell. The abnormalities common to each culture were a derivative chromosome 2 (or possibly an inversion), a chromosome 15 trisomy, a derivative chromosome 21, and a chromosome 22 derivative or monosomy. The karyotypes of each culture are shown in Table 1. The TK6-2 cell line was used for FISH controls because it had approximately 46 chromosomes and the fewest number of anomalies.

TK6 slides were examined under brightfield microscopy after freezing to ensure high numbers of mitotic figures, and then stained with FITC pan-centromeric FISH probes and a DAPI counterstain with Antifade mounting media. Slides were scanned with the DAPI filter at 10x or 20x to find prophase, metaphase, and anaphase nuclei and nearby interphase nuclei were counted. All cells observed had centromeric staining consistent with the expected locations of centromeres (Figure 13). Twenty cells from three slides were counted for fluorescent signals, including interphases, prophases, and metaphases. I found a mean of 44 centromeric staining regions, with a standard error of 0.7, less than 2% of the mean (Table 2).



<b>Culture</b>	<b>Derivative/Inversion</b>	<b>Trisomy</b>	<b>Monosomy</b>	<b>Absent</b>
TK6-2	2, 21	15	22	N/A
TK6-46	2, 21, 22*	15, 22*	14, 19	N/A
TK6-48	2, 21, 22*, 6*	15, 22*, 6*	4, 7, 9, 11, 16, 19	14, 18, X, Y

\*Two normal copies and one inverted copy were found.

Table 1: TK6 culture karyotypes by Dr. Anne Higgins at Brigham and Women's Hospital. TK6-2 was used for control FISH studies because it had the fewest abnormalities and approximately 46 chromosomes per cell.

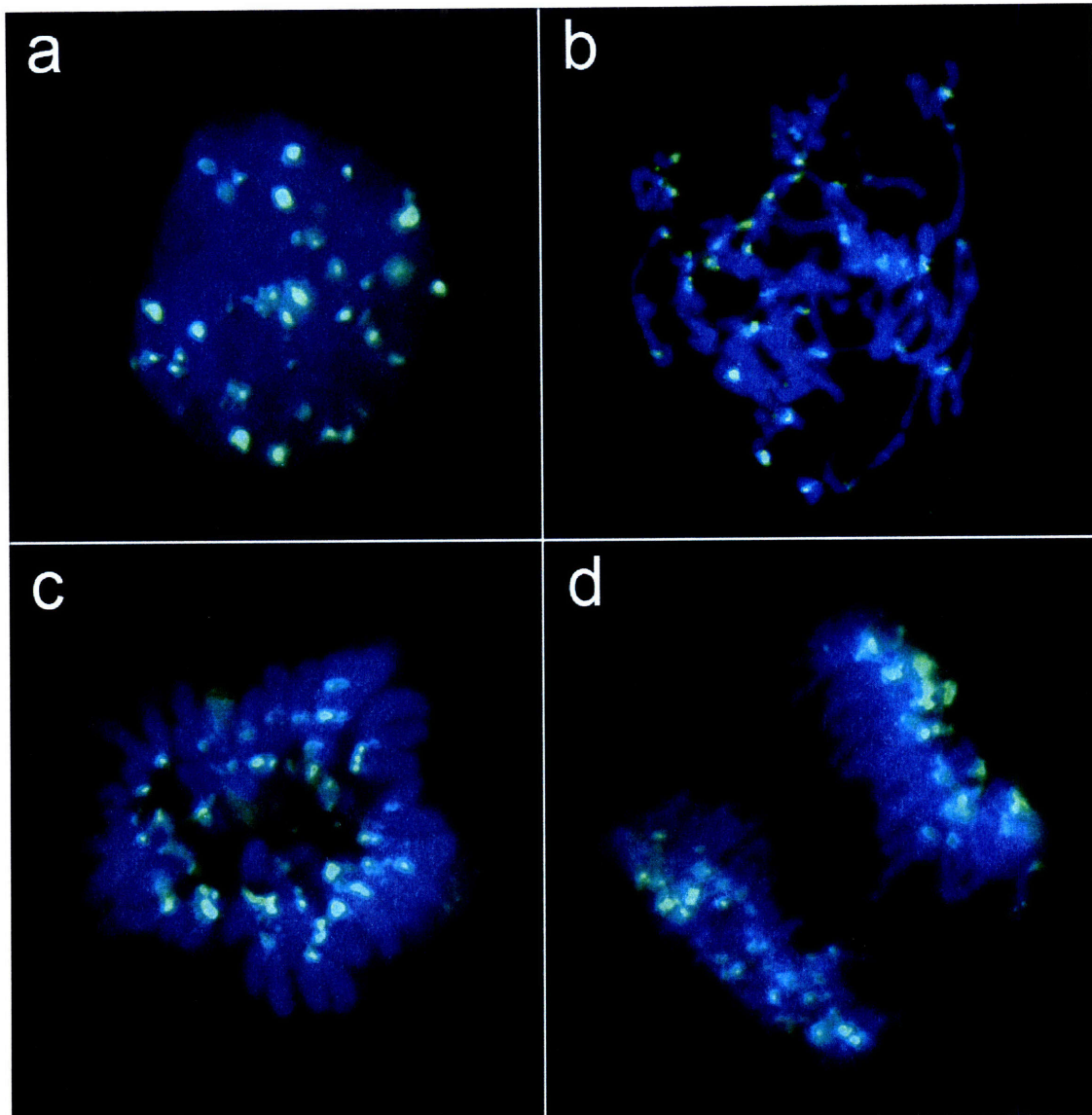


Figure 13: Pan-centromeric FISH staining of TK6 mitotic figures. Centromeric regions represented in green (FITC filter) and DAPI stain of DNA represented in blue (DAPI filter). Staining region counts and locations were consistent with what is expected for human centromeres. a) interphase, 44 centromeric staining regions; b) prophase, 38 centromeric staining regions; c) metaphase, 49 centromeric staining regions; d) anaphase, 39 and 37 centromeric staining regions (left to right).

#### 4.1.1.2 Human Fetal Gut and Spinal Cord

My second set of centromeric controls were mitotic cells in the same fetal samples as the metakaryotic cells. Fetal tissue gut and spinal cord slides were examined under brightfield microscopy to ensure proper spreading, and then stained with FITC pan-centromeric FISH probes and a DAPI counterstain with Antifade mounting media. Slides were scanned with the DAPI filter at 20x to find areas of bright and even staining that contained metakaryotic nuclei. Metaphase and interphase nuclei nearby were counted. Twenty-five cells from three slides (Two slides of 12 week fetal gut and one of 7 week fetal spinal cord) were counted for fluorescent signals including interphases and metaphases. I found a mean of 41.4 centromeric staining regions, with a standard error of 0.9, ~2% of the mean (Table 2).

#### 4.1.2 Telomere Counts

##### 4.1.2.1 Human Fetal Gut and Spinal Cord

My telomeric controls were mitotic cells in the same fetal samples as the metakaryotic cells. Fetal tissue gut slides were examined under brightfield microscopy to ensure proper spreading, and then stained with FITC pan-telomeric FISH probes and a DAPI counterstain with Antifade mounting media. Slides were scanned with the DAPI filter at 20x to find areas of bright and even staining that contained metakaryotic nuclei. Interphase nuclei nearby were counted. Twenty-five cells from two slides were counted for fluorescent signals. I found a mean of 42.7 centromeric staining regions, with a standard error of 0.7, less than 2% of the mean (Table 2).

#### 4.1.3 Whole Chromosomes

##### 4.1.3.1 Human Lymphoblastoid Cell Line (TK6)

Whole chromosome FISH proved much more difficult in the fetal samples than either pan-centromeric or pan-telomeric FISH. I practiced with several different chromosomes on TK6 cells until I felt comfortable with the technique, and even then it was extremely difficult to get signal in fetal samples.

##### 4.1.3.2 Human Fetal Gut

My chromosome 6 controls were mitotic cells in the same fetal samples as the metakaryotic cells. Fetal tissue gut slides were examined under brightfield microscopy to ensure proper spreading, and then stained with FITC whole chromosome 6 FISH probes and a DAPI counterstain with Antifade mounting media. Slides were scanned with the DAPI filter at 20x to find areas of bright and even staining that contained metakaryotic nuclei. Interphase nuclei nearby were observed. Approximately 60% of eukaryotic cells counted had two bright signals. The other 40% either showed one signal or a diffuse mass of signal across the cell, unable to be quantified.

## 4.2 Metakaryotic Cells

Metakaryotic cells were identified with the DAPI filter at 20x magnification. Single, extrasyncytial metakaryotic cells were identified by their 3-dimensional bell shaped nuclei (by changing focal planes), condensed ring around the rim of the bell, and the autofluorescent balloon projecting from the mouth of the bell. Dividing metakaryotic cells were identified by their 3-dimensional bell shaped nuclei (by changing focal planes), the cup-from-cup orientation, and the autofluorescent syncytium that surrounded them.

### 4.2.1 Centromeres

#### 4.2.1.1 Human Fetal Gut and Spinal Cord

Fetal tissue gut and spinal cord slides were examined under brightfield microscopy to ensure proper spreading, and then stained with FITC pan-centromeric FISH probes and a DAPI counterstain with Antifade mounting media. Slides were scanned with the DAPI filter at 20x to find areas of bright and even staining that contained metakaryotic nuclei. Single, extrasyncytial metakaryotic nuclei had compact, discrete centromeric signals in all cells found. In contrast, metakaryotes in active cup-from-cup divisions had centromeres that looked decondensed, or diffuse (Figure 14). Because the signals were diffuse and the nuclei overlapped in the cup-from-cup orientation, it was not possible to count numbers of centromeric signals in dividing metakaryotes.

The centromeric staining regions in single, extrasyncytial metakaryotic nuclei were countable. Twenty nuclei from three slides were counted and gave a mean of 22.9, with a standard error of 0.6, ~3% of the mean (Table 2, Figure 15). The centromeric signals were often in pairings, or “doublets,” which were counted as one region (Figure 14a). Two signals were considered a doublet if the distance between the signals was less than the diameter of the smaller signal (~0.5 microns), the signals were pointed in the same direction (signals often had “tails”), and were of similar size and fluorescent intensity. Previous studies of fluorescent signal pairing used similar methods to determine whether signals were paired (Zalensky et al., 1997; Scherthan et al., 1996).

#### 4.2.1.2 Human Colon FAPC Adenomas and Adenocarcinomas

FAPC adenoma and adenocarcinoma slides were examined under brightfield microscopy to ensure proper spreading, and then stained with FITC pan-centromeric FISH probes and a DAPI counterstain with Antifade mounting media. Slides were scanned with the DAPI filter at 20x to find areas of bright and even staining that contained metakaryotic nuclei. I found slightly higher numbers of centromeric staining regions, with a mean of 27.9, and a standard error of 0.6, ~3% of the mean (Table 2). The staining regions were also often in doublets, which were counted as one region.

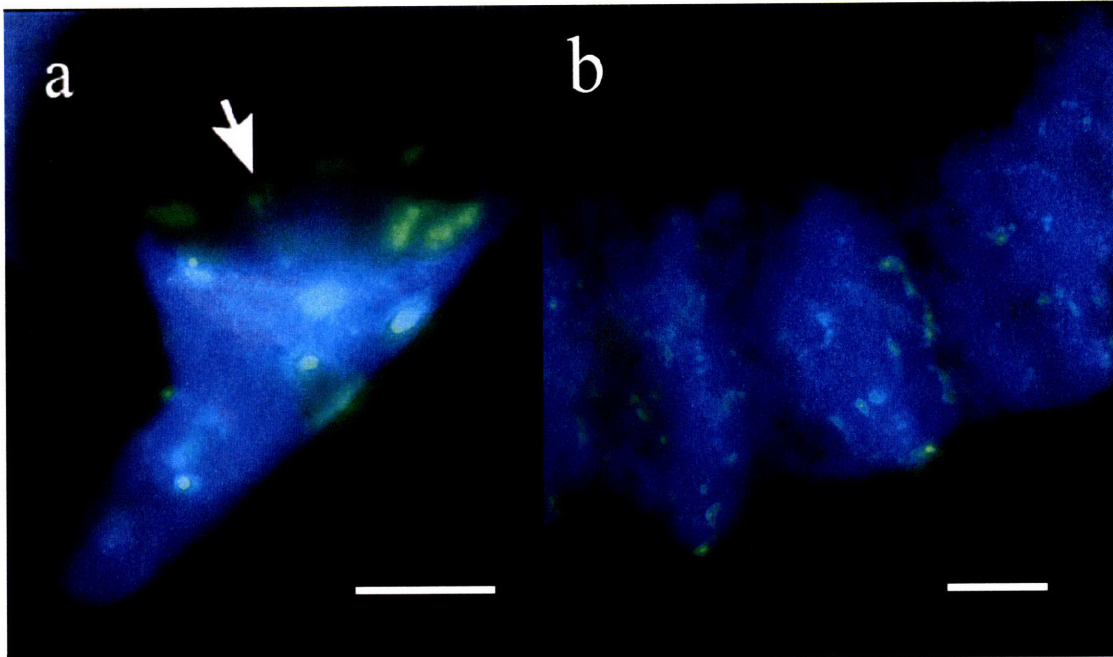


Figure 14: FISH staining of human centromeric regions in single and dividing metakaryotic nuclei. Centromeric regions represented in green (FITC filter) and DAPI stain of DNA represented in blue (DAPI filter). a) Single, extrasyncytial metakaryotic nuclei from 12 week fetal gut have discrete, condensed centromeric staining regions. The arrow shows a pairing, or doublet, of two centromeric signals. b) Actively dividing metakaryotic nuclei from 7 week fetal spinal cord have diffuse, centromeric staining, possibly indicating a necessary DNA decondensation step in its amitotic “cup-from-cup” division process. Bars = 5  $\mu\text{m}$ .

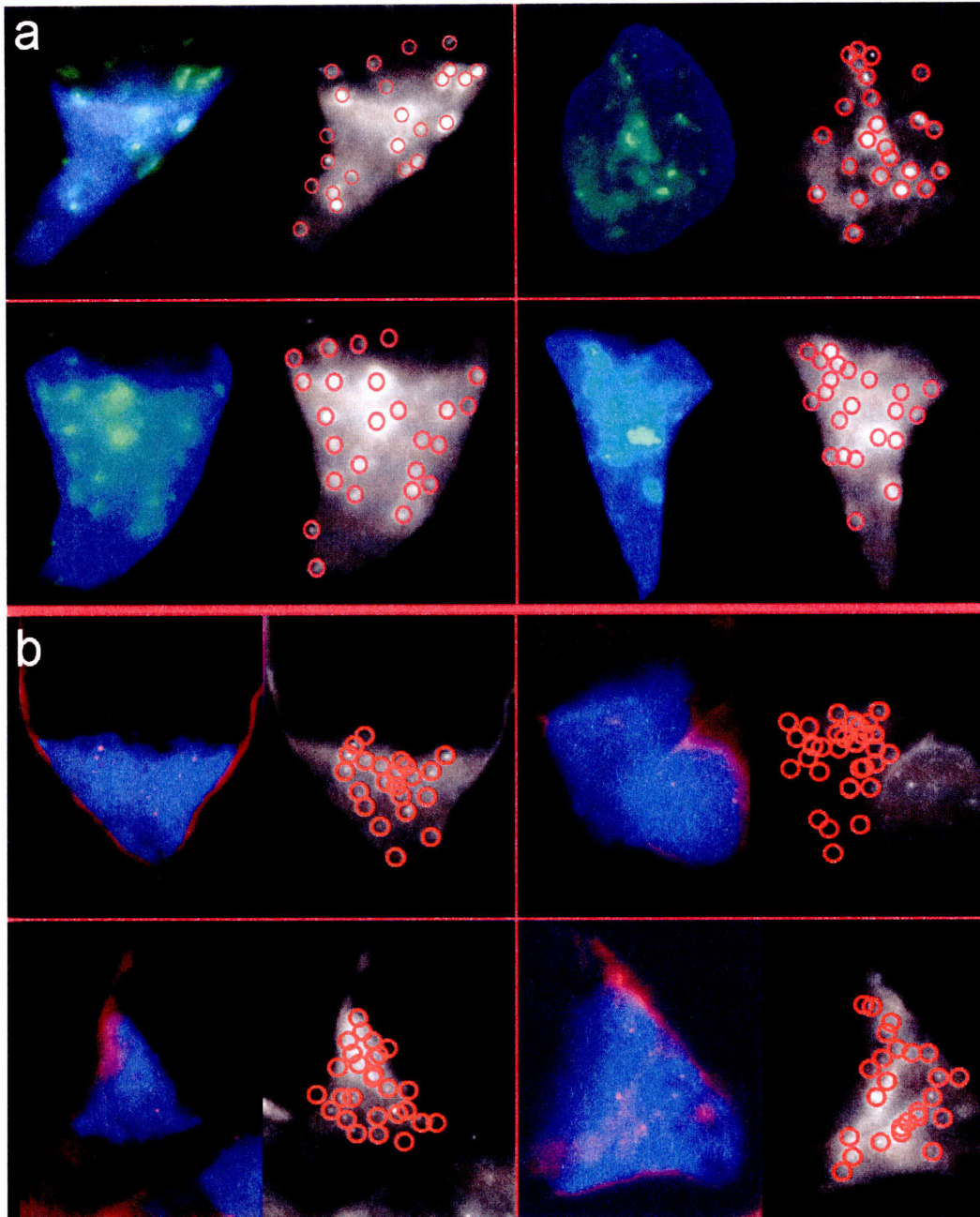


Figure 15: Counts of centromeric and telomeric staining regions in single, extrasyncytial, fetal metakaryotic nuclei. Centromeric regions represented in green (FITC filter), telomeric regions represented in fuchsia (FITC filter) and DAPI stain of DNA represented in blue (DAPI filter). Each panel contains a color overlay of the DAPI and FITC filters and a black and white version of the image with all staining regions circled in red. a) Pan-centromeric FISH staining of single, extrasyncytial metakaryotic nuclei from 12 week fetal gut with 23, 24, 25, and 22 staining regions (top left, top right, bottom left, bottom right). b) Pan-telomeric FISH staining of single, extrasyncytial metakaryotic nuclei from 12 week fetal gut with 22, 28, 25, and 24 staining regions (top left, top right, bottom left, bottom right).

## 4.2.2 Telomere Counts

### 4.2.2.1 Human Fetal Gut and Spinal Cord

Fetal tissue gut slides were examined under brightfield microscopy to ensure proper spreading, and then stained with FITC pan-telomeric FISH probes and a DAPI counterstain with Antifade mounting media. Slides were scanned with the DAPI filter at 20x to find areas of bright and even staining that contained metakaryotic nuclei. Fourteen single, extrasyncytial metakaryotic nuclei were counted from two slides. I found a mean of 24.2, with a standard error of 0.6, less than 3% of the mean (Table 2, Figure 15). The telomeric signals were also seen as doublets, which were counted as one region, or occasionally triplets, which were counted as two regions. Two signals were considered a doublet if the distance between the signals was less than the diameter of the smaller signal (~0.3 microns) and the signals were of similar fluorescent intensity. All telomere signals were of similar size and were observed as compact points (no tails or diffusions).

## 4.2.3 Whole Chromosomes

### 4.2.3.1 Human Fetal Gut

Fetal tissue gut slides were examined under brightfield microscopy to ensure proper spreading, and then stained with FITC whole chromosome 6 FISH probes and a DAPI counterstain with Antifade mounting media. Slides were scanned with the DAPI filter at 20x to find areas of bright and even staining that contained metakaryotic nuclei. Single, extrasyncytial metakaryotic nuclei showed two signals, one at the bottom of the bell and one at the rim (Figure 16).

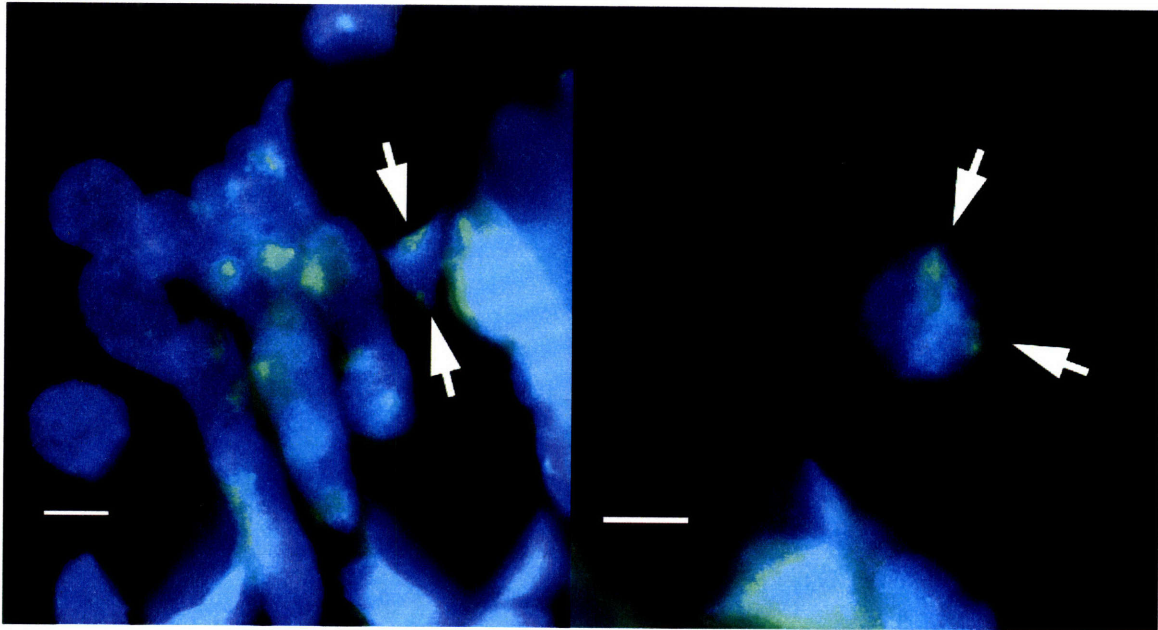


Figure 16: FISH staining of chromosome 6 in 12 week human fetal gut. Both images show metakaryotic nuclei with two chromosome 6 staining regions, denoted by arrows, one at the top of the bell, and one at the bottom. The presence of two staining regions suggests that either homologous pairing is not taking place along the regions of chromosome 6 between the centromeres and telomeres, or that the p and q arms of chromosome 6 are separated across the bell (See Figure 19). Bars = 10  $\mu$ m.



### 4.3 Statistics

Centromere and telomere counts were performed by random walk in bell-shaped nuclei in proto-organs, adenomas, and adenocarcinomas. Counts within specimen were continued for at least five images or until the SE of the mean count was within 3% of the mean.

To determine if there was a statistical difference between the centromere or telomere counts of one group compared to another, the means were compared to see if they lay within two or three standard deviations of each other. All numbers used in calculations can be found in Table 2.

To reject the null hypothesis:  $\mu(\text{group A}) = \mu(\text{group B})$ ,  
 $|\mu(\text{group A}) - \mu(\text{group B})| - 3\sqrt{[V(\text{group A}) + V(\text{group B})]} > 0$

The first null hypothesis tested was that metakaryotic nuclei and the control eukaryotic nuclei had the same number of centromeric signals. Metakaryotic nuclei were compared to both the TK6 control group and the fetal control group. The null hypothesis was rejected for both comparisons using the 99% confidence limits.

TK6 cells and fetal metakaryotic cells (centromeres):

$$|(44.0 - 22.9)| - 3\sqrt{(11.0 + 6.2)} = 8.7 \gg 0$$

Fetal eukaryotic/mitotic cells and fetal metakaryotic cells (centromeres):

$$|(41.4 - 22.9)| - 3\sqrt{(19.2 + 6.2)} = 3.3 \gg 0$$

The second null hypothesis was that metakaryotic nuclei and the control fetal eukaryotic nuclei had the same number of telomeric signals. This was also rejected using the 99% confidence limits.

Fetal eukaryotic/mitotic cells and fetal metakaryotic cells (telomeres):

$$|(42.7 - 24.2)| - 3\sqrt{(12.0 + 4.9)} = 6.2 \gg 0$$

The counts for carcinomic metakaryotes were slightly higher than those in fetal tissues, so the hypothesis that metakaryotic nuclei in fetal tissue and carcinomic tissue had the same number of centromeric signals was tested. Using the 99% confidence limits, this hypothesis could not be rejected, so there is no significant statistical difference in the number of centromeric signals in fetal and carcinomic metakaryotic nuclei.

Fetal metakaryotic cells and cancerous metakaryotic cells (centromeres):

$$|(22.9 - 27.9)| - 3\sqrt{(6.2 + 2.4)} = -3.8 < 0$$

Table 2: FISH centromeric and telomeric staining counts and statistics.

## Centromeres

Sample	Cell Type	Number Cells (n)	Range of total signals	Mean ( $\mu$ )	Variance (V)	Standard Deviation (SD)	Standard Error (SE)
TK6 Cell Line	Eukaryotic/mitotic	20	38-50	44.0	11.0	3.3	0.7
Fetal gut and spinal cord	Eukaryotic/mitotic	25	35-50	41.4	19.2	4.4	0.9
Fetal gut and spinal cord	Metakaryotic	20	19-29	22.9	6.2	2.5	0.6
Adult FAPC polyps and tumors	Metakaryotic	7	25-29	27.9	2.4	1.6	0.6

## Telomeres

Sample	Cell Type	Number Cells (n)	Range of total signals	Mean ( $\mu$ )	Variance (V)	Standard Deviation (SD)	Standard Error (SE)
Fetal gut and spinal cord	Eukaryotic/mitotic	24	38-51	42.7	12.0	3.5	0.7
Fetal gut and spinal cord	Metakaryotic	14	21-28	24.2	4.9	2.2	0.6

#### 4.4 Sources of Error

Since I was working in two dimensions, signals were undoubtedly not identified when they had the same x and y coordinates, but different z coordinates (on top of one another).

Therefore, a certain amount of undercounting is an expected error. To determine if this could affect my numbers enough to question my findings, I took four 3-dimensional z-stack images of metakaryotic nuclei from our new microscope and counted the number of centromeric staining regions. The numbers of 19, 20, 21 and 23 are typical counts and fit within one and a half standard deviations of the mean.

Most studies note that FISH staining is incomplete for telomeres, and only 75% to 82% of telomeres are stained in human cells (Henderson et al., 1996; Weierich et al., 2003). Given the means of 42.7 and 24.2 for eukaryotic and metakaryotic fetal nuclei, respectively, and the previous studies on telomeres in humans, it seems that telomeres are overwhelmingly associated in eukaryotic interphase cells. Therefore, the probability of a doublet where neither telomere is seen is  $0.2^2$ , or 0.04, so the true mean may actually be closer to 44.4 staining regions per cell for eukaryotic fetal interphase cells. The probability of a tetrad where neither telomere is seen is approximately  $0.2^4$ , or less than 0.002, which would not change the mean for metakaryotic cells.

To determine the exact number of centromeric and telomeric staining regions in each group with greater statistical confidence, more cells could be counted, but the basic difference between ~23 and ~46 staining regions would remain unchanged. My goal was to determine if there was a statistical difference in the numbers of centromeric and telomeric signals between eukaryotes and metakaryotes, which I have. However, given the fact that telomeres in human interphase cells seem to associate into 12, 25, 38, 51, 78, or 91 telomeric staining regions per cell (See section 2.2.1.1.), and the fact that dividing bells display decondensed centromere sequences, it is certainly possible that some bells (especially syncytial) might have different numbers of telomere staining regions.

## 5. DISCUSSION

### 5.1 Control Results

The goal of this thesis was to study the organization of metakaryotic cells. Given their unusual method of division, we expected their organization to differ from eukaryotic cells, so it was necessary to look at control nuclei to have a comparison.

Interphase, prophase, and metaphase nuclei were counted for each control group, as well as spherical, cigar-shaped, and ovoid nuclei in the fetal mitotic cells. Metaphase nuclei had numbers ranging from 42 to 47, which are consistent with previous studies of FISH pan-centromeric stains in human metaphase cells (Fomina et al., 2000). Studies of human eukaryotic interphase cells have various numbers of centromeric staining regions per cell (Weierich et al., 2003), which would explain the variation in my numbers (lymphoblastoid cell line TK6,  $\mu = 44$ ,  $V = 11.0$ ; mitotic nuclei of the fetal tissues studied,  $\mu = 41.3$ ,  $V = 19.2$ ).

Telomeric staining regions were counted in spherical, cigar-shaped, and ovoid interphase nuclei in the fetal mitotic cells. Mitotic nuclei from fetal tissues exhibited approximately 43 telomeric staining regions ( $\mu = 42.7$ ). Most studies note that FISH staining is incomplete for telomeres, and only 75% to 82% of telomeres are stained (Henderson et al., 1996; Weierich et al., 2003). This is assumed to be because telomeres have large protein complexes that may prevent access to telomeric DNA. Given a mean of 42.7, it seems that telomeres are overwhelmingly paired in embryonic interphase cells, which would mean that the probability of a doublet where neither telomere is seen is 0.04. Taking this into account, the mean may actually be closer to 44 staining regions per cell. Studies of human eukaryotic interphase cells also have a wide variety of number of telomeric staining regions (See section 2.2.1.1.), which would explain the variation in my numbers ( $V = 12.0$ ).

### 5.2 Metakaryotic Centromere and Telomere Organization

All single, extrasyncytial metakaryotic cells observed had centromere staining regions that were all or mostly condensed, so they appeared as discrete points. However, actively dividing metakaryotic nuclei (in a “cup-from-cup” division orientation) had centromere staining regions that appeared diffuse, or decondensed, as strings. This suggested that, contrary to eukaryotic cells (in which DNA is condensed for separation), during the division process in metakaryotic cells, the DNA is decondensed in areas that exist as heterochromatin during interphase. This supported a theory of Professor Thilly’s that the amitotic division of metakaryotic cells might involve the separation of the genome into four (or more) single stranded molecules to allow an epigenetically unmodified genomic copy to be transferred to the daughter cell. For a separation of this kind, the genome would likely need to be fully or almost fully decondensed, as observed in the dividing metakaryotic cells.

Contrary to the control nuclei, approximately 23 centromeric staining regions were observed in single, extrasyncytial fetal metakaryotic nuclei, about half of expected ( $\mu = 22.9$ ,  $SE = 0.6$ ). The null hypothesis that the number of centromere staining regions in metakaryotic nuclei was not statistically different from the number of centromere staining regions eukaryotic

nuclei was tested and rejected with more than 99% confidence (See section 4.3). Single, extrasyncytial metakaryotic cells also had several signal pairings, or doublets, per nuclei, which were counted as one region. This led to the hypothesis that perhaps the metakaryotic genome was organized into homologous chromosome pairs, which seems likely since the eukaryotic genome is homologously paired during meiosis in humans and mice, and during the entire cell cycle in yeast and Dipteran insects. It seems reasonable that some of these same mechanisms may be used for centromeric pairing in metakaryotic nuclei.

To test the hypothesis that metakaryotic chromosomes were homologously paired, FISH with pan-telomeric probes was performed on fetal metakaryotic nuclei, with the expectation that a mean of 43 (controls) to 46 telomeres would be observed per nuclei, depending on the state of telomere-protein interactions in metakaryotic cells. Unexpectedly, in fetal metakaryotic cells, the number of telomeres was also about half of what was found in controls, about 23 telomeric staining regions per metakaryotic nuclei ( $\mu = 24.2$ ,  $SE = 0.6$ ). Interestingly enough, previous studies of human eukaryotic interphase cells show a peak at about 23 telomeric staining regions (See section 2.2.1.1.). The fact that FISH telomere staining is usually about 80% efficient would not affect the mean to any significant degree, considering telomeres seem to be associating in tetrads very much like the ones that exist in human sperm (Figure 5). That would mean the possibility of a tetrad where none of the telomeres are visible is less than 0.2%. I rejected the null hypothesis that the number of telomere signals was the same in metakaryotes and eukaryotes with 99% confidence (See section 4.3). Professor Thilly pointed out that telomeres associating into tetrads supports his previous hypothesis of end-joining of the telomeres of chromosomes to make circular genomic segments (Figure 18).

Since these cells are also likely candidates for the lineage of tumors, I looked at centromere signals in interphase cells in both colon polyps and colon tumors. The numbers of centromere signals were slightly increased ( $\mu = 27.9$ ,  $SE = 0.6$ ) as would be expected for cells that have a higher degree of aneuploidy. However, a statistical analysis yielded no significant difference in the number or distribution of signals between polyp and tumor metakaryotic nuclei and fetal metakaryotic nuclei (See section 4.3).

As this was my first time performing FISH on non-cultured cells, Dr. Gostjeva contacted a colleague of hers in the Netherlands experienced in FISH staining, Professor Firouz Darroudi, who heads the Cytogenetics Unit in the University of Leiden Medical Center. Dr. J. Fomina in Professor Darroudi's lab confirmed my counts of 23 centromeres and 23 telomeres in human metakaryotic nuclei and the existence of doublets (Figure 17).

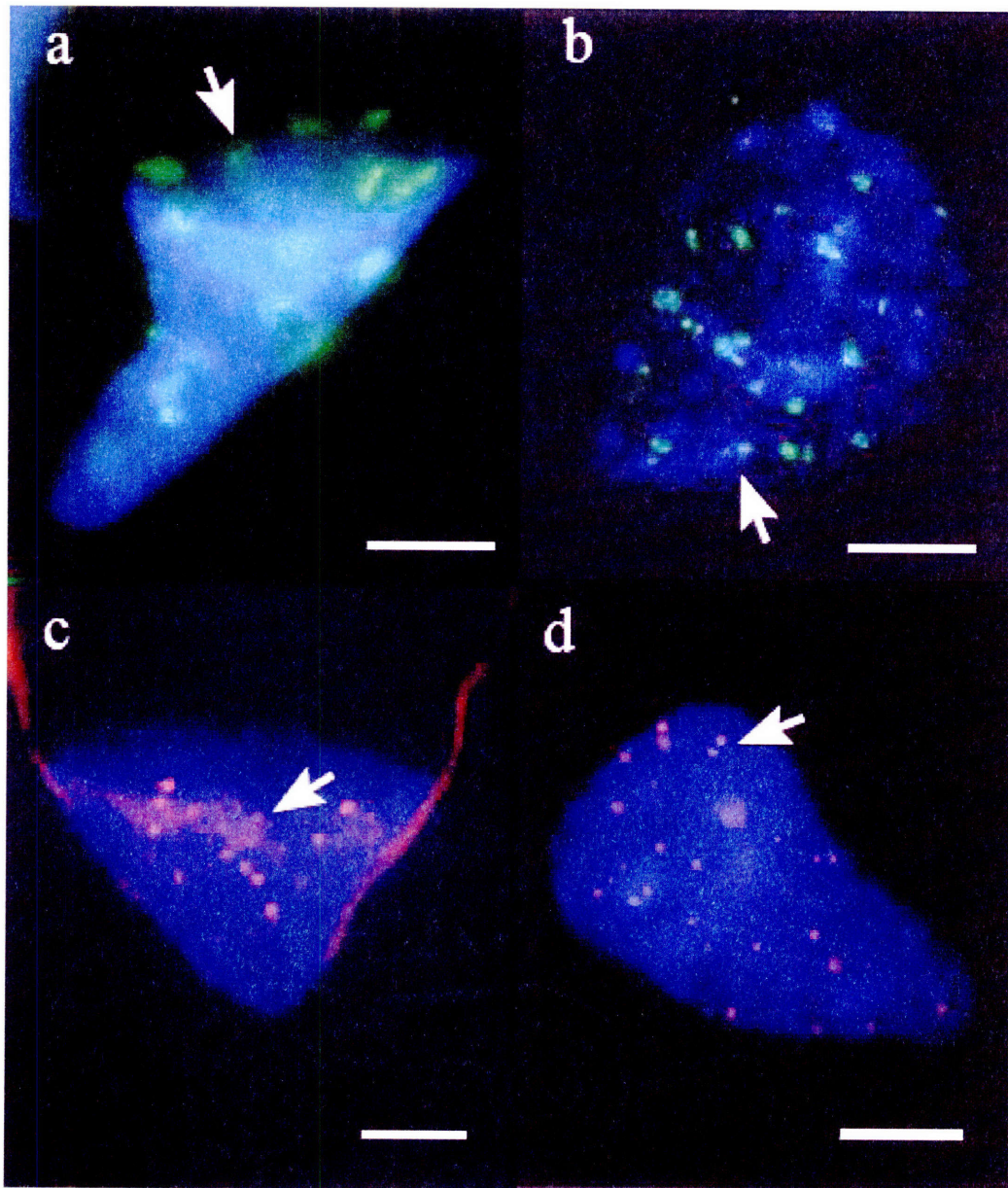


Figure 17: Confirmation of FISH results using antibody staining of human centromeric and telomeric regions in metakaryotic cells. Dr. J. Fomina in the lab of Professor Firouz Darroudi used human centromere and telomere antibodies to confirm my counts of 23 centromeres and 23 telomeres. a) FISH staining and b) fluorescent antibody staining of human centromeres in bell-shaped nuclei reveal typical counts of 22 and 23 centromeric staining regions, represented in green. Note the presence of doublets, shown by the arrows, which we count as one centromeric staining region. c) FISH staining and d) fluorescent antibody staining of human telomeres in bell-shaped nuclei reveal counts of 20 and 24 telomeric staining regions, represented in fuchsia. Note the presence of doublets, which are counted as one telomeric staining region. DAPI stain of DNA is represented in blue. Photomicrographs b) and d) by Dr. J. Fomina and Professor Firouz Darroudi. Reproduced from Gostjeva et al., 2008 (manuscript in preparation).

### 5.3 Metakaryotic Genome Models and Additional Findings

The previous work on adult maintenance stem cells (or cells mimicking their behavior in cell cultures) retaining a single, continuous genomic copy (Cairns, 2006; Merok et al., 2002; Karpowicz et al., 2005; Shinin et al., 2006), along with observations of a double-ring structure around the “mouth” of metakaryotic nuclei, and my observation of approximately 23 centromeric staining regions and 23 telomeric staining regions per nuclei, point to a unified theory of metakaryotic organization and division. Amitotic division of metakaryotic cells might involve separation of the genome into four (or more) single stranded molecules to allow segregation of epigenetically unmodified and untranscribed new DNA strands into the daughter cell. If this is the case, the genomes of bell-shaped nuclei could be organized as several sets of circular molecules, consisting of several chromosomes joined at their telomeric ends for ease in separating all Watson strands from all Crick strands. These molecules could orient themselves in pairs with sets of centromeres and telomeres overlapping (Figure 18). In the theorized models, the centromeres are paired homologously and the telomeres are both paired homologously and joined with another telomere pair. It could be an intrachromosomal pair to make circular chromosomes, or an interchromosomal pair to make a daisy chain of chromosomes. The daisy chain could be each haploid genome as one circular molecule, or several chains of differing length. Any combination of telomeric ends would account 23 telomere regions seen in metakaryotic cells and any centromere pairing would account for the 23 centromere regions observed. These pairing models would also account for the occasional doublets seen in both centromere and telomere signals.

The next question was whether it was likely homologous pairing was taking place along the entire chromosome length. So I used a whole chromosome probe for chromosome 6 in bell shaped nuclei and found two separate signals, one at the rim, and one at the bottom of the bell (Figure 16). Professor Firouz Darroudi’s lab in Leiden also found two signals with a probe for chromosome 18, confirming my findings. This doesn't necessarily rule out the possibility of homologous pairing along the length of the chromosome, but if that is the case, the chromosome would have to be separated into two separate regions, possibly the p and q arms with the centromeres joined in the middle (Figure 19). Another possibility is that the two signals shown represent the maternal and paternal copies, perhaps with the centromere and telomere signals joined in the middle between the two.

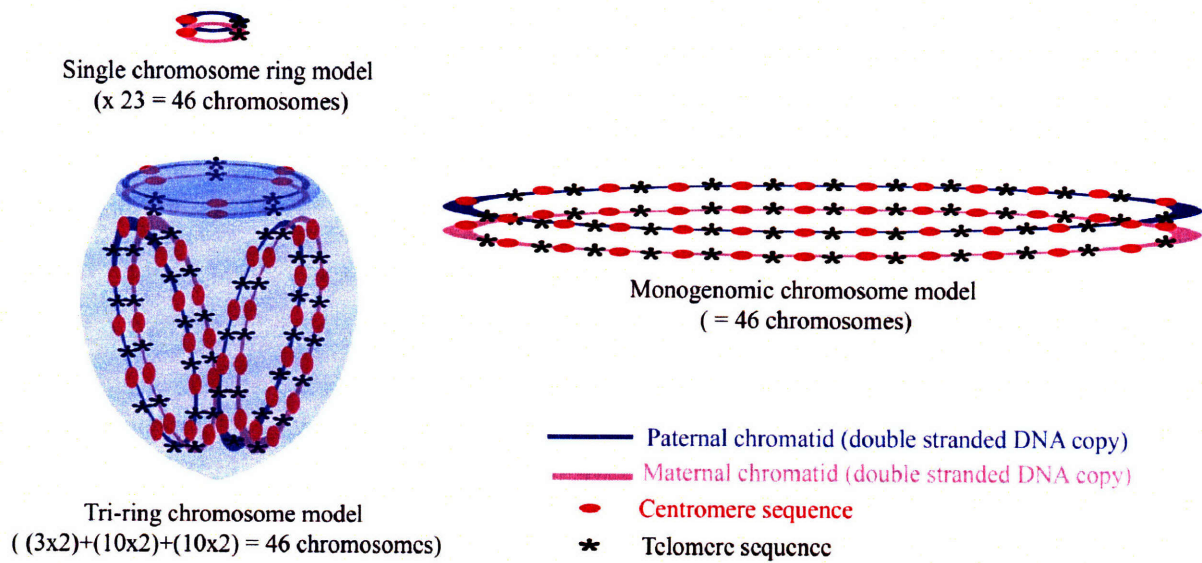


Figure 18: Possible models for metakaryotic genomic organization. Blue and pink represent the paternal and maternal genomes, respectively. Red dots and asterisks represent centromeres and telomeres, respectively. Centromeres are paired homologously and telomeres are both paired homologously and joined with another telomere pair. The three different models show how single chromosomes, several chromosomes, or all chromosomes could be joined to create the 23 centromere and 23 telomere staining regions observed. The tri-ring model is shown inside a metakaryotic nucleus to show possible positioning.



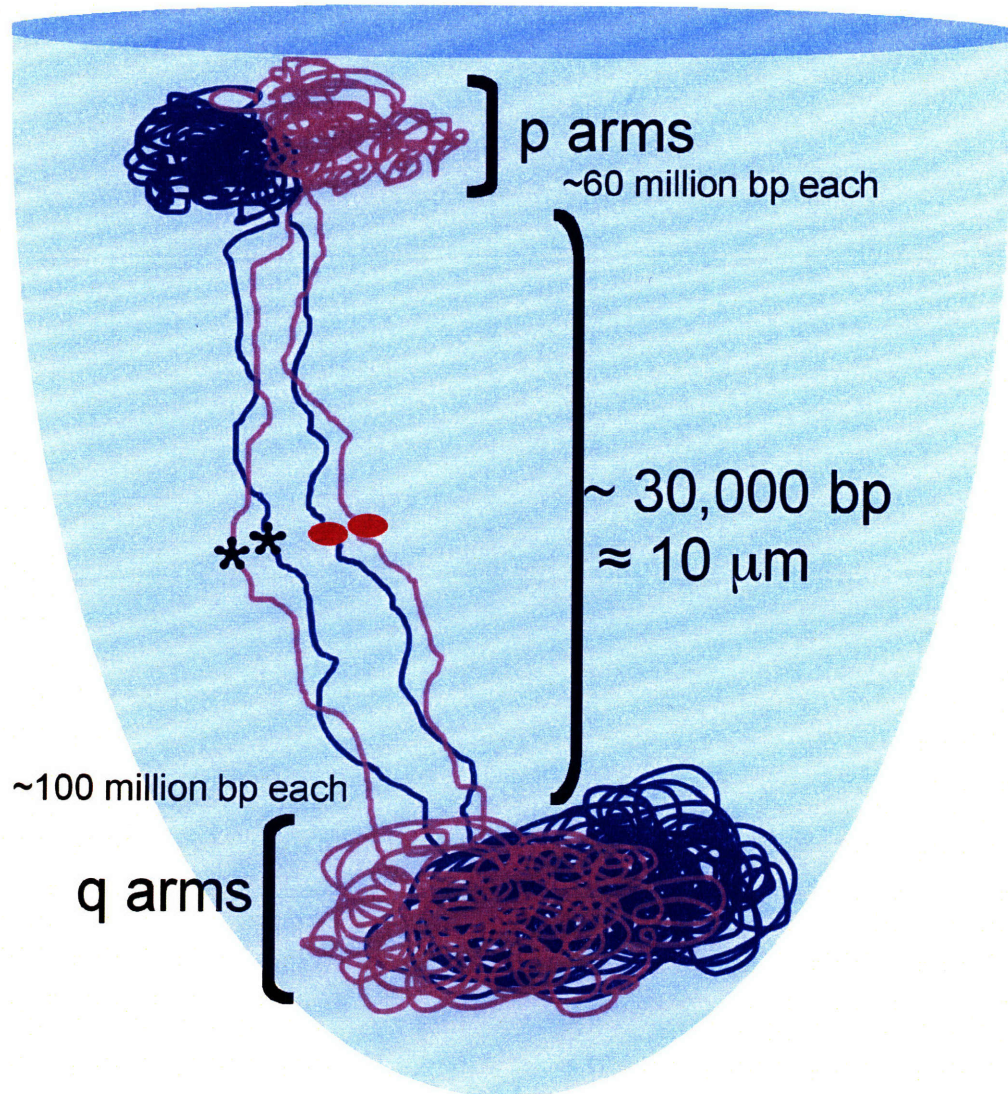


Figure 19: Model for possible homologous pairing of chromosome 6 in metakaryotes. Dark blue and pink represent the paternal and maternal copies of chromosome 6, respectively. Each chromosome 6 copy is a continuous ring, connected at its telomeric regions, and homologously paired. The DNA sequences proximal and distal to the centromeres and telomeres are shown as completely decondensed DNA to illustrate the possibility that only about 30,000 base pairs would be necessary to separate the p and q arms of chromosome 6 across a metakaryotic nucleus.

## 5.4 Related Studies

Another interesting question is how groupings of four telomeres are achieved. Telomeres have been found to bind using their repeat DNA sequences in various conformations. Human telomeres have a single stranded overhang of about 300 base pairs (Wright et al., 1997) that forms G-quadruplex structures (Figure 2) in sodium and potassium solutions (Makita et al., 2005). These structures can form from different strands, so it is possible that the telomeric overhangs might be joined in metakaryotic cells. Telomeric binding proteins such as TRF1 and TRF2, members of the shelterin complex, which bind double stranded telomeric repeats in humans (Court et al., 2005; de Lange et al., 2005) and TEBP $\alpha$  and TEBP $\beta$ , which have been shown to mediate the formation of the G-tetraplex structures in vivo (Paeschke et al., 2005), may also be involved in either the formation or maintenance of such structures. In our own lab, Dr. Per Olaf Ekstrøm followed up on the idea that the repeat DNA sequences of telomeres might be joined. He found a peritelomeric sequence for chromosome X that was not found anywhere else in the genome, and used it as a PCR primer. When tissue sections of about 20% metakaryotic cells were amplified, a set of 400-500 bp sequences was created, but adult human cheek cells yielded no signal (Figure 20). These findings suggest that metakaryotic cells are forming telomeric bridges, possibly without protein interactions, just by joining their overhang ends (Figure 21).

Dr. Elena Gostjeva has done subsequent work related to the theories put forth in this thesis. Using acridine orange, which stains double stranded DNA green and single stranded DNA orange, she found that dividing bells go through a single stranded intermediate before becoming fully double stranded (Figure 22). This agrees with my observations of actively dividing bells with decondensed centromere signals, and is evidence for a division process in which Watson and Crick strands separate into single stranded molecules to provide the daughter cell with epigenetically unmodified and untranscribed new DNA strands.

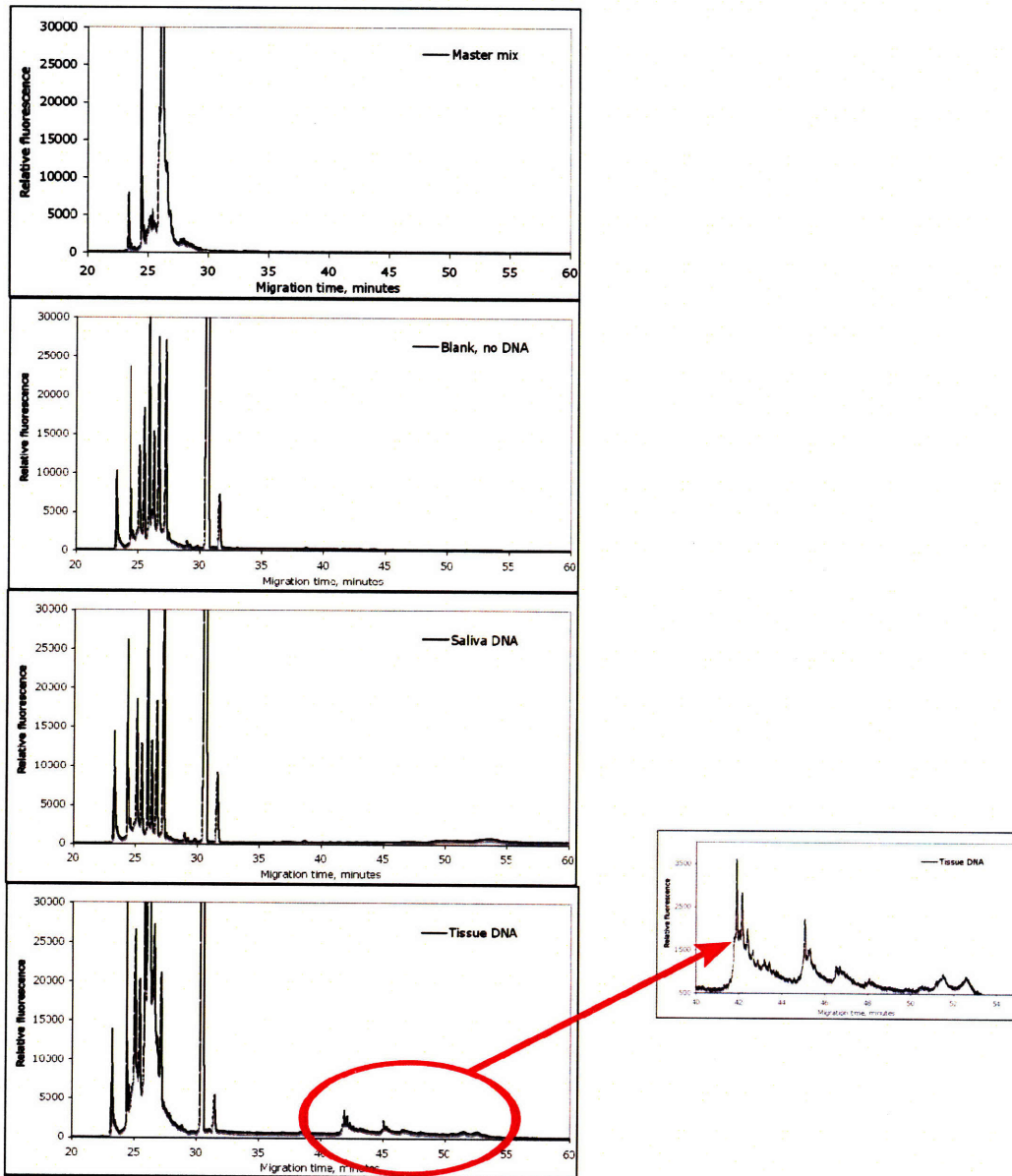


Figure 20: Capillary electrophoresis results from telomere bridging PCR studies by Dr. Per Olaf Ekstrøm using peritelomeric primers. From top to bottom on the left, capillary electrophoresis runs of Master Mix alone, PCR amplified Master Mix, PCR amplified DNA from adult saliva, and PCR amplified DNA from fetal tissue with ~20% metakaryotic cells, with an enlargement of the 400-500 base pair PCR products seen only in fetal tissue. The absence of those products in all but the fetal sample supports the idea that telomeres are combining to produce continuous double stranded DNA sequences in metakaryotic, but not eukaryotic cells.

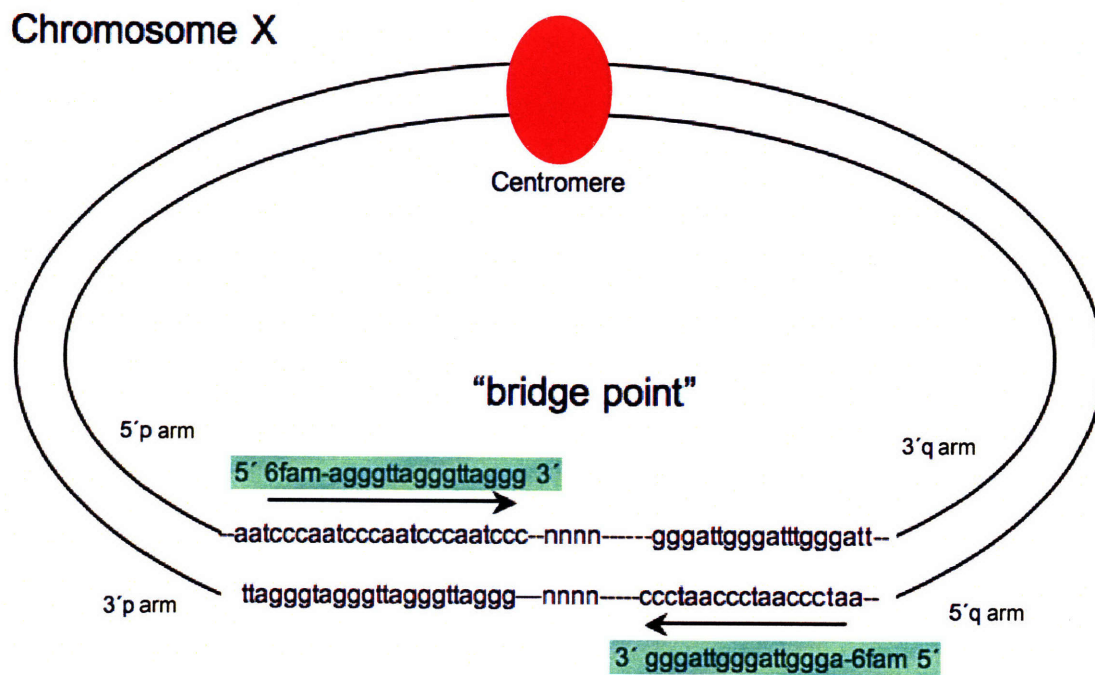


Figure 21: Model of human telomere bridging by Dr. Per Olaf Ekstrøm. The red circle represents the centromere region. The arrows and the boxed DNA sequences represent the peritelomeric primers used for the telomere bridging PCR experiments. Chromosome X is one of the only chromosomes whose p and q telomere regions have been fully sequenced. The 3' telomeric overhangs of the p and q arms could be combined as shown to produce a continuous double stranded DNA sequence that could be amplified by the primers.

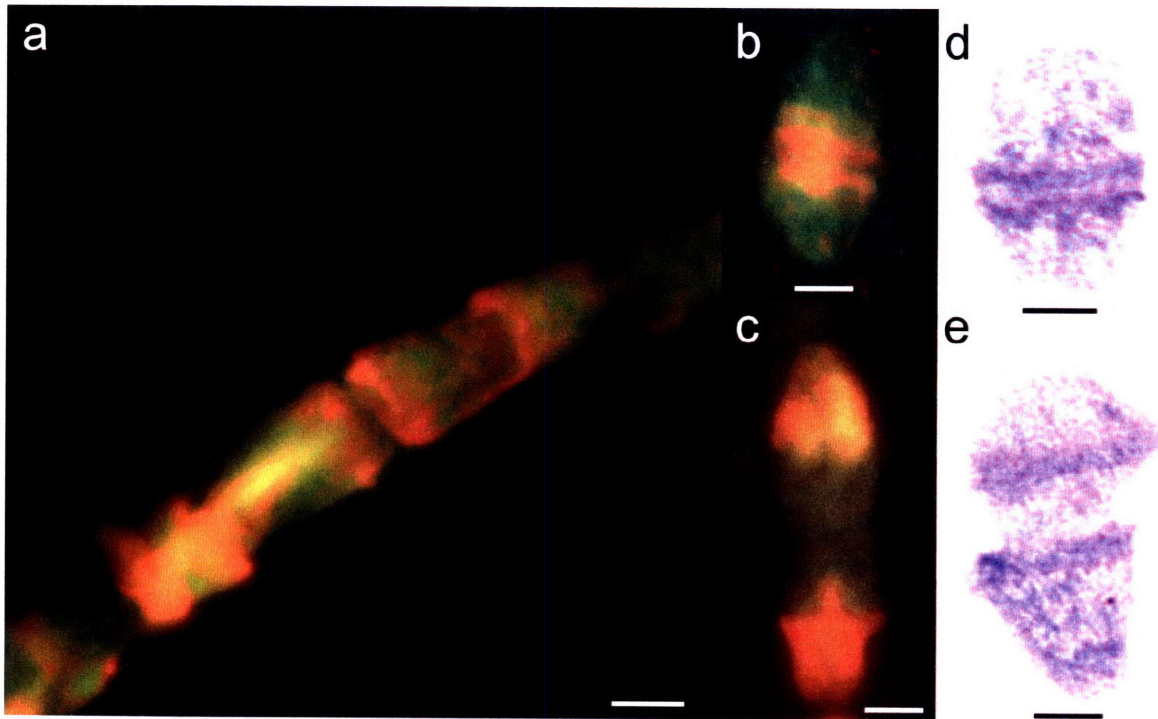


Figure 22: Single stranded DNA studies on dividing metakaryotic nuclei conducted by Dr. Elena Gostjeva. Panels a), b), and c) show acridine orange staining of dividing metakaryotic nuclei. d) and e) show Feulgen staining of dividing metakaryotic nuclei. Green and orange stain show double stranded DNA and single stranded DNA, respectively. a) Metakaryotic nuclei dividing “cup-from-cup” inside syncytia. b) Beginning of metakaryotic division “à ceinture” showing single stranded DNA near the condensed “belt” in the middle. c) Middle of metakaryotic division “à ceinture” showing two new nuclei almost entirely single stranded. d) Beginning of metakaryotic division “à ceinture” showing condensed DNA “belt” in the middle. e) Middle of metakaryotic division “à ceinture” showing two new nuclei pulling away from each other. Bars = 5  $\mu\text{m}$ . Unpublished image used with permission of Dr. Elena Gostjeva. Photomicrographs and histology provided by Dr. Elena Gostjeva.

## 5.5 Mutation in Metakaryotes from Human Development

To add to these contributions, I participated in mutation research that turned out to have particular significance to the metakaryotic research presented in the previous sections. I was one of a four person team that used allele specific PCR to measure five separate point mutations in multiple microanatomical sections from fifteen human lungs (Sudo et al., 2006; Sudo et al., 2008, manuscript under review). We found that cigarette smoking did not affect any of the five mutation fractions measured (Figure 23a). A linear regression analysis for mutant fractions as a function of age (38 to 76 years) computed a slope near zero, which indicates mutant fractions do not increase with age (Figure 23b). Both these findings were surprising, and led us to examine the data more closely.

An analysis of mutant cluster sizes showed that the number of mutant clusters is linearly distributed in a log graph with regard to the size of the cluster (Figure 24b). This is what would be expected for the growth of early mutant colonies, as pointed out by the Luria-Delbruck experiments, and is consistent with the hypothesis that the point mutations measured occurred at a constant high mutation rate per stem cell doubling throughout the fetal-juvenile period. This data also agreed with previous data of mitochondrial point mutations in human lung by Dr. Hillary Coller (2005) that showed the same relationship between mutant cluster size and number of mutant clusters and estimated the human lung turnover unit as 32 cells (Figure 24a).

The idea that point mutations occur during the fetal-juvenile period is supported by other studies. Brash (1991) found that sunlight did not increase the number of recognizable mutant TP53 colonies in adult skin. All new mutations occurred in sun-exposed juvenile skin. Andrea Kim, formerly of the Thilly Lab, organized and analyzed data for specific translocations in blood lymphocytes and found steady increases during, and then constant levels after, the juvenile period. Based on the concordance of high mutation rates and metakaryotic cells behaving as stem cells in the fetal-juvenile period we hypothesize that the high mutation rates are a phenotypic quality of metakaryotic cells. Dr. Gostjeva's acridine orange work sheds light on the high mutation rate found for these cells, since single stranded DNA has high mutation rates because no excision repair can take place.

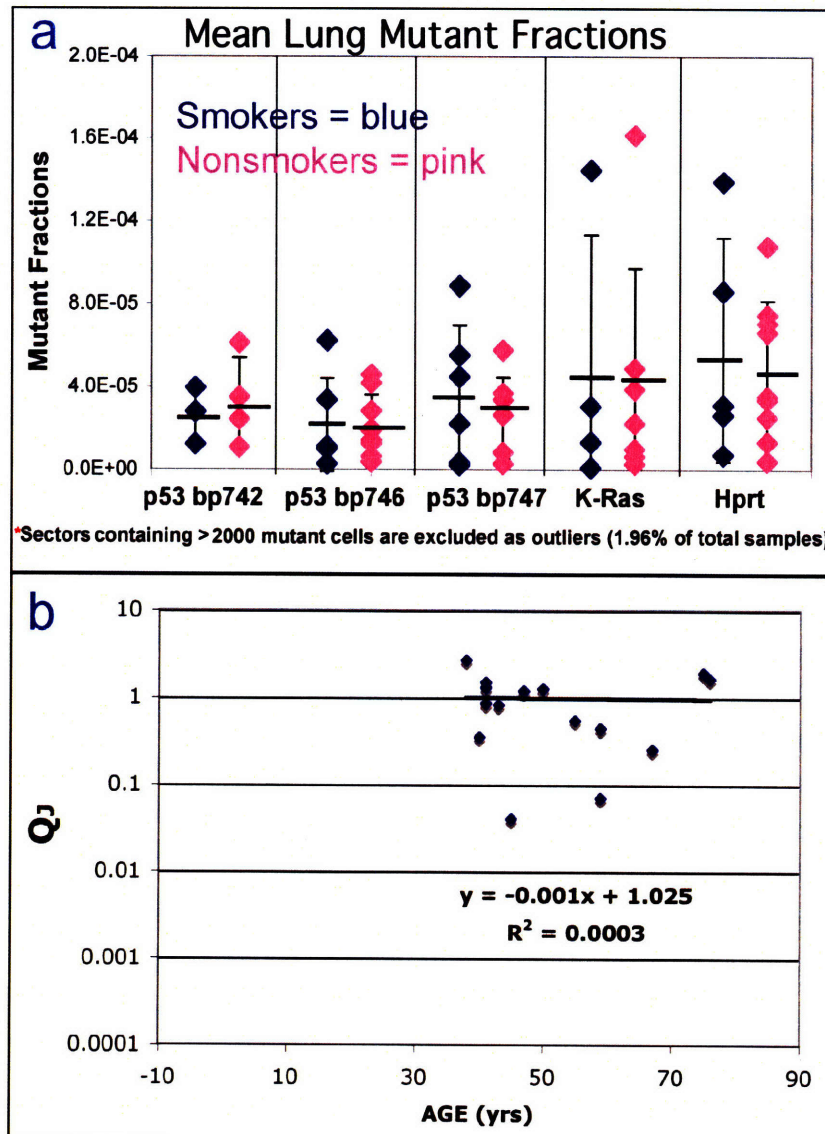


Figure 23: Lung mutant fractions as a function of smoking status and age. a) Distributions of the mean mutant fractions among lungs of smokers (dark blue diamonds on left) and non-smokers (pink diamonds on right) for TP53 base pairs 742, 746, and 747, K-ras base pair 35, and Hprt base pair 508 (from left to right). Each diamond represents a mean mutant fraction of an individual lung, the short black bars indicate the grand mean for each target, and the error bars indicate two standard deviations. Note there is no difference between the mutant fractions in the lungs of smokers and non-smokers. b)  $\log_{10}$  of normalized mean mutant fractions for lungs as a function of age. Solid line indicates the linear regression computed with a slope near zero, which indicates mutant fractions are the same for ages 38 to 76. Reproduced with permission from the Ph.D. thesis of Dr. Hiroko Sudo and Sudo et al., 2008 (manuscript under review).

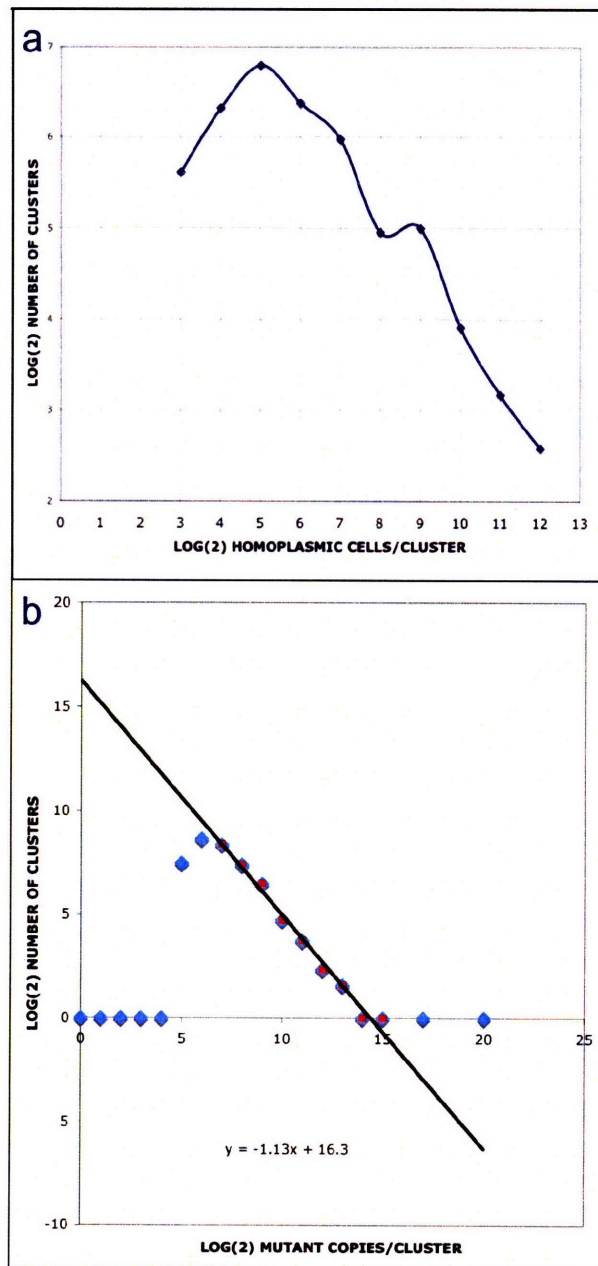


Figure 24: Analyses of lung mutant cluster numbers and sizes in mitochondrial and nuclear DNA. a) Analysis of the  $\log_2$  of the number of mitochondrial point mutation clusters as a function of  $\log_2$  number of cells per cluster. The data came from assays of 17 point mutations in mitochondria of human adult lung epithelium by Dr. Hillary Collier (Collier et al., 2005). A maximum is observed at 32 cells that serves as an estimation of the size of a turnover unit in the human lung. b) Analysis of the  $\log_2$  of the number of nuclear point mutation clusters as a function of  $\log_2$  number of cells per cluster. The data came from assays of 5 nuclear point mutations in human adult lung epithelium by Dr. Hiroko Sudo. The  $\log_2$  number of clusters decreases exponentially with  $\log_2$  cluster size with a slope near 1. This is consistent with the hypothesis that mutant clusters originated as stem cell mutations during the fetal-juvenile period. Reproduced with permission from Sudo et al., 2008 (manuscript under review).



## CONCLUSION

Metakaryotic cells, which display a shibboleth of stem cells (asymmetrical nuclear fission) in human organogenesis and carcinogenesis, divide using an unusual amitotic process in which DNA synthesis and nuclear separation occur concurrently. To discover how metakaryotic genomes are organized, this thesis focused on using FISH to determine the numbers and locations of DNA sequences commonly used to study genomic organization: centromeres, telomeres, and chromosomes.

Based on my results, several new facts about human metakaryotic organization are now known. Actively dividing metakaryotes have decondensed, or diffuse, centromeric staining regions which suggests that one of the steps in metakaryotic division is decondensation of centromeres or possibly all DNA (completely the opposite of mitotic division). Single, extrasyncytial metakaryotic cells have approximately 23 centromeric and 23 telomeric condensed, or discrete, staining regions, many of which are seen as doublets, or pairs. The number of centromeric staining regions (half of expected) indicates pairing of centromeres, and the number of telomeric staining regions (one quarter of expected) indicates both pairing and joining of telomeres to form tetrads. The presence of doublets that look similar to centromere pairings during meiosis and spermatogenesis suggests possible homologous pairing of centromeres. However, staining of individual chromosomes gives two separate signals, suggesting if there is homologous pairing, it is probably not along the chromosomal regions between centromeres and telomeres. Metakaryotic cells in polyps and carcinomas have slightly higher centromeric signals, expected since those cells often display aneuploidy, but no significant statistical difference in the number of centromeric signals.

My findings suggest a possible model of metakaryotic organization in which the maternal and paternal genomes are organized as one or more paired, continuous circular molecules by telomere joining. Dr. Per Olaf Ekstrøm's PCR studies of telomere bridging in tissues containing metakaryotic cells have provided further evidence for this model.

Human lung mutation studies I participated in prior to my imaging studies supply evidence that all mutations found in adults are created during the fetal-juvenile period. Dr. Elena Gostjeva's single stranded DNA assays determined that dividing metakaryotic cells have a single stranded intermediate stage, which would explain the high mutation rates found in the lung studies, and suggest the cells I researched in the mutation and imaging studies may be the very same.

The results in this thesis are original and important contributions to the fields of stem cell physiology and human development, and immediate further investigation of the organization, division, mutation, and repair of DNA sequences in these metakaryotic cells is needed. The metakaryotic research in the Thilly lab has the potential to transform the fields of stem cell, human development, and cancer research, and I have been fortunate to participate in it.

## REFERENCES

- Alcobia, I., Dilao, R. and Parreira, L. (2000). Spatial associations of centromeres in the nuclei of hematopoietic cells: evidence for cell-type-specific organizational patterns. *Blood*. 95(5): 1608-15.
- Alcobia, I., Quina, A. S., Neves, H., Clode, N. and Parreira, L. (2003). The spatial organization of centromeric heterochromatin during normal human lymphopoiesis: evidence for ontogenically determined spatial patterns. *Exp Cell Res*. 290(2): 358-69.
- Amrichova, J., Lukasova, E., Kozubek, S. and Kozubek, M. (2003). Nuclear and territorial topography of chromosome telomeres in human lymphocytes. *Exp Cell Res*. 289(1): 11-26.
- Bass, H. W., Riera-Lizarazu, O., Ananiev, E. V., Bordoli, S. J., Rines, H. W., Phillips, R. L., Sedat, J. W., Agard, D. A. and Cande, W. Z. (2000). Evidence for the coincident initiation of homolog pairing and synapsis during the telomere-clustering (bouquet) stage of meiotic prophase. *J Cell Sci*. 113 ( Pt 6): 1033-42.
- Beil, M., Durschmied, D., Paschke, S., Schreiner, B., Nolte, U., Bruel, A. and Irinopoulou, T. (2002). Spatial distribution patterns of interphase centromeres during retinoic acid-induced differentiation of promyelocytic leukemia cells. *Cytometry*. 47(4): 217-25.
- Beil, M., Fleischer, F., Paschke, S. and Schmidt, V. (2005). Statistical analysis of the three-dimensional structure of centromeric heterochromatin in interphase nuclei. *J Microsc*. 217(Pt 1): 60-8.
- Bolzer, A., Kreth, G., Solovei, I., Koehler, D., Saracoglu, K., Fauth, C., Muller, S., Eils, R., Cremer, C., Speicher, M. R. and Cremer, T. (2005). Three-dimensional maps of all chromosomes in human male fibroblast nuclei and prometaphase rosettes. *PLoS Biol*. 3(5): e157.
- Borden, J. and Manuelidis, L. (1988). Movement of the X chromosome in epilepsy. *Science*. 242(4886): 1687-91.
- Boyle, S., Gilchrist, S., Bridger, J. M., Mahy, N. L., Ellis, J. A. and Bickmore, W. A. (2001). The spatial organization of human chromosomes within the nuclei of normal and emerin-mutant cells. *Hum Mol Genet*. 10(3): 211-9.
- Brash, D. E., Rudolph, J. A., Simon, J. A., Lin, A., McKenna, G. J., Baden, H. P., Halperin, A. J. and Ponten, J. (1991). A role for sunlight in skin cancer: UV-induced p53 mutations in squamous cell carcinoma. *Proc Natl Acad Sci U S A*. 88(22): 10124-8.
- Bridger, J. M., Boyle, S., Kill, I. R. and Bickmore, W. A. (2000). Re-modelling of nuclear architecture in quiescent and senescent human fibroblasts. *Curr Biol*. 10(3): 149-52.

- Burge, S., Parkinson, G. N., Hazel, P., Todd, A. K. and Neidle, S. (2006). Quadruplex DNA: sequence, topology and structure. *Nucleic Acids Res.* 34(19): 5402-15.
- Cairns, J. (1975). Mutation selection and the natural history of cancer. *Nature.* 255(5505): 197-200.
- Cairns, J. (2006). Cancer and the immortal strand hypothesis. *Genetics.* 174(3): 1069-72.
- Carvalho, C., Pereira, H. M., Ferreira, J., Pina, C., Mendonca, D., Rosa, A. C. and Carmo-Fonseca, M. (2001). Chromosomal G-dark bands determine the spatial organization of centromeric heterochromatin in the nucleus. *Mol Biol Cell.* 12(11): 3563-72.
- Cervantes, M. D., Coyne, R. S., Xi, X. and Yao, M. C. (2006). The condensin complex is essential for amitotic segregation of bulk chromosomes, but not nucleoli, in the ciliate *Tetrahymena thermophila*. *Mol Cell Biol.* 26(12): 4690-700.
- Chambeyron, S. and Bickmore, W. A. (2004). Chromatin decondensation and nuclear reorganization of the HoxB locus upon induction of transcription. *Genes Dev.* 18(10): 1119-30.
- Cheng, K. and Zou, C. (2005). 3-D physical models of amitosis (cytokinesis). *Med Hypotheses.* 64(1): 88-91.
- Chubb, J. R., Boyle, S., Perry, P. and Bickmore, W. A. (2002). Chromatin motion is constrained by association with nuclear compartments in human cells. *Curr Biol.* 12(6): 439-45.
- Coller, H. A., Khrapko, K., Herrero-Jimenez, P., Vatland, J. A., Li-Sucholeiki, X. C. and Thilly, W. G. (2005). Clustering of mutant mitochondrial DNA copies suggests stem cells are common in human bronchial epithelium. *Mutat Res.* 578(1-2): 256-71.
- Court, R., Chapman, L., Fairall, L. and Rhodes, D. (2005). How the human telomeric proteins TRF1 and TRF2 recognize telomeric DNA: a view from high-resolution crystal structures. *EMBO Rep.* 6(1): 39-45.
- Cremer, M., Kupper, K., Wagler, B., Wizelman, L., von Hase, J., Weiland, Y., Kreja, L., Diebold, J., Speicher, M. R. and Cremer, T. (2003). Inheritance of gene density-related higher order chromatin arrangements in normal and tumor cell nuclei. *J Cell Biol.* 162(5): 809-20.
- Cremer, M., von Hase, J., Volm, T., Brero, A., Kreth, G., Walter, J., Fischer, C., Solovei, I., Cremer, C. and Cremer, T. (2001). Non-random radial higher-order chromatin arrangements in nuclei of diploid human cells. *Chromosome Res.* 9(7): 541-67.
- Cremer, T., Cremer, C., Baumann, H., Luedtke, E. K., Sperling, K., Teuber, V. and Zorn, C. (1982). Rabl's model of the interphase chromosome arrangement tested in Chinese hamster cells by premature chromosome condensation and laser-UV-microbeam experiments. *Hum*

Genet. 60(1): 46-56.

Cremer, T., Cremer, M., Dietzel, S., Muller, S., Solovei, I. and Fakan, S. (2006). Chromosome territories--a functional nuclear landscape. *Curr Opin Cell Biol.* 18(3): 307-16.

Cremer, T., Kurz, A., Zirbel, R., Dietzel, S., Rinke, B., Schrock, E., Speicher, M. R., Mathieu, U., Jauch, A., Emmerich, P., Scherthan, H., Ried, T., Cremer, C. and Lichter, P. (1993). Role of chromosome territories in the functional compartmentalization of the cell nucleus. *Cold Spring Harb Symp Quant Biol.* 58: 777-92.

Cremer, T., Tesin, D., Hopman, A. H. and Manuelidis, L. (1988). Rapid interphase and metaphase assessment of specific chromosomal changes in neuroectodermal tumor cells by in situ hybridization with chemically modified DNA probes. *Exp Cell Res.* 176(2): 199-220.

Croft, J. A., Bridger, J. M., Boyle, S., Perry, P., Teague, P. and Bickmore, W. A. (1999). Differences in the localization and morphology of chromosomes in the human nucleus. *J Cell Biol.* 145(6): 1119-31.

de Lange, T. (1992). Human telomeres are attached to the nuclear matrix. *EMBO J.* 11(2): 717-24.

de Lange, T. (1994). Activation of telomerase in a human tumor. *Proc Natl Acad Sci U S A.* 91(8): 2882-5.

de Lange, T. (2005). Shelterin: the protein complex that shapes and safeguards human telomeres. *Genes Dev.* 19(18): 2100-10.

Devilee, P., Slagboom, P., Cornelisse, C. J. and Pearson, P. L. (1986). Sequence heterogeneity within the human alphoid repetitive DNA family. *Nucleic Acids Res.* 14(5): 2059-73.

Ding, D. Q., Yamamoto, A., Haraguchi, T. and Hiraoka, Y. (2004). Dynamics of homologous chromosome pairing during meiotic prophase in fission yeast. *Dev Cell.* 6(3): 329-41.

Ding, X., Xu, R., Yu, J., Xu, T., Zhuang, Y. and Han, M. (2007). SUN1 is required for telomere attachment to nuclear envelope and gametogenesis in mice. *Dev Cell.* 12(6): 863-72.

Essers, J., van Cappellen, W. A., Theil, A. F., van Drunen, E., Jaspers, N. G., Hoeijmakers, J. H., Wyman, C., Vermeulen, W. and Kanaar, R. (2005). Dynamics of relative chromosome position during the cell cycle. *Mol Biol Cell.* 16(2): 769-75.

Ferreira, M. G. and Cooper, J. P. (2004). Two modes of DNA double-strand break repair are reciprocally regulated through the fission yeast cell cycle. *Genes Dev.* 18(18): 2249-54.

Flint, J., Bates, G. P., Clark, K., Dorman, A., Willingham, D., Roe, B. A., Micklem, G., Higgs, D. R. and Louis, E. J. (1997). Sequence comparison of human and yeast telomeres identifies structurally distinct subtelomeric domains. *Hum Mol Genet.* 6(8): 1305-13.

- Fomina, J., Darroudi, F., Boei, J. J. and Natarajan, A. T. (2000). Discrimination between complete and incomplete chromosome exchanges in X-irradiated human lymphocytes using FISH with pan-centromeric and chromosome specific DNA probes in combination with telomeric PNA probe. *Int J Radiat Biol.* 76(6): 807-13.
- Fomina, J., Darroudi, F. and Natarajan, A. T. (2001). Accurate detection of true incomplete exchanges in human lymphocytes exposed to neutron radiation using chromosome painting in combination with a telomeric PNA probe. *Int J Radiat Biol.* 77(12): 1175-83.
- Fraser, P. and Bickmore, W. (2007). Nuclear organization of the genome and the potential for gene regulation. *Nature.* 447(7143): 413-7.
- Funabiki, H., Hagan, I., Uzawa, S. and Yanagida, M. (1993). Cell cycle-dependent specific positioning and clustering of centromeres and telomeres in fission yeast. *J Cell Biol.* 121(5): 961-76.
- Gasser, S. M. (2002). Visualizing chromatin dynamics in interphase nuclei. *Science.* 296(5572): 1412-6.
- Gerlich, D., Beaudouin, J., Kalbfuss, B., Daigle, N., Eils, R. and Ellenberg, J. (2003). Global chromosome positions are transmitted through mitosis in mammalian cells. *Cell.* 112(6): 751-64.
- Gerlich, D. and Ellenberg, J. (2003). Dynamics of chromosome positioning during the cell cycle. *Curr Opin Cell Biol.* 15(6): 664-71.
- Gilbert, N. and Allan, J. (2001). Distinctive higher-order chromatin structure at mammalian centromeres. *Proc Natl Acad Sci U S A.* 98(21): 11949-54.
- Gilchrist, S., Gilbert, N., Perry, P. and Bickmore, W. A. (2004). Nuclear organization of centromeric domains is not perturbed by inhibition of histone deacetylases. *Chromosome Res.* 12(5): 505-16.
- Gostjeva, E. V. and Thilly, W. G. (2005). Stem cell stages and the origins of colon cancer: a multidisciplinary perspective. *Stem Cell Rev.* 1(3): 243-51.
- Gostjeva, E. V., Zukerberg, L., Chung, D. and Thilly, W. G. (2006). Bell-shaped nuclei dividing by symmetrical and asymmetrical nuclear fission have qualities of stem cells in human colonic embryogenesis and carcinogenesis. *Cancer Genet Cytogenet.* 164(1): 16-24.
- Gotta, M., Laroche, T., Formenton, A., Maillet, L., Scherthan, H. and Gasser, S. M. (1996). The clustering of telomeres and colocalization with Rap1, Sir3, and Sir4 proteins in wild-type *Saccharomyces cerevisiae*. *J Cell Biol.* 134(6): 1349-63.
- Griffith, J. D., Comeau, L., Rosenfield, S., Stansel, R. M., Bianchi, A., Moss, H. and de

- Lange, T. (1999). Mammalian telomeres end in a large duplex loop. *Cell*. 97(4): 503-14.
- Hanaoka, S., Nagadoi, A. and Nishimura, Y. (2005). Comparison between TRF2 and TRF1 of their telomeric DNA-bound structures and DNA-binding activities. *Protein Sci*. 14(1): 119-30.
- Hardie, D. C., Gregory, T. R. and Hebert, P. D. (2002). From pixels to picograms: a beginners' guide to genome quantification by Feulgen image analysis densitometry. *J Histochem Cytochem*. 50(6): 735-49.
- Henderson, S., Allsopp, R., Spector, D., Wang, S. S. and Harley, C. (1996). In situ analysis of changes in telomere size during replicative aging and cell transformation. *J Cell Biol*. 134(1): 1-12.
- Hiraoka, Y., Agard, D. A. and Sedat, J. W. (1990). Temporal and spatial coordination of chromosome movement, spindle formation, and nuclear envelope breakdown during prometaphase in *Drosophila melanogaster* embryos. *J Cell Biol*. 111(6 Pt 2): 2815-28.
- Jabs, E. W. and Persico, M. G. (1987). Characterization of human centromeric regions of specific chromosomes by means of alphoid DNA sequences. *Am J Hum Genet*. 41(3): 374-90.
- Jackson, D. A. (2003). The principles of nuclear structure. *Chromosome Res*. 11(5): 387-401.
- Karpowicz, P., Morshead, C., Kam, A., Jarvis, E., Ramunas, J., Cheng, V. and van der Kooy, D. (2005). Support for the immortal strand hypothesis: neural stem cells partition DNA asymmetrically in vitro. *J Cell Biol*. 170(5): 721-32.
- Kupper, K., Kolbl, A., Biener, D., Dittrich, S., von Hase, J., Thormeyer, T., Fiegler, H., Carter, N. P., Speicher, M. R., Cremer, T. and Cremer, M. (2007). Radial chromatin positioning is shaped by local gene density, not by gene expression. *Chromosoma*. 116(3): 285-306.
- Kuroda, M., Tanabe, H., Yoshida, K., Oikawa, K., Saito, A., Kiyuna, T., Mizusawa, H. and Mukai, K. (2004). Alteration of chromosome positioning during adipocyte differentiation. *J Cell Sci*. 117(Pt 24): 5897-903.
- Laroche, T., Martin, S. G., Gotta, M., Gorham, H. C., Pryde, F. E., Louis, E. J. and Gasser, S. M. (1998). Mutation of yeast Ku genes disrupts the subnuclear organization of telomeres. *Curr Biol*. 8(11): 653-6.
- Leslie, A. G., Arnott, S., Chandrasekaran, R. and Ratliff, R. L. (1980). Polymorphism of DNA double helices. *J Mol Biol*. 143(1): 49-72.
- Levy, J. A., Buell, D. N., Creech, C., Hirshaut, Y. and Silverberg, H. (1971). Further characterization of the WI-L1 and WI-L2 lymphoblastoid lines. *J Natl Cancer Inst*. 46(3): 647-54.

- Levy, J. A., Virolainen, M. and Defendi, V. (1968). Human lymphoblastoid lines from lymph node and spleen. *Cancer*. 22(3): 517-24.
- Lew, D. J., Burke, D. J. and Dutta, A. (2008). The immortal strand hypothesis: how could it work? *Cell*. 133(1): 21-3.
- Li, L. (2007). Does 'immortal DNA strand' exist in 'immortal' stem cells? *Cell Res*. 17(10): 834-5.
- Liber, H. L. and Thilly, W. G. (1982). Mutation assay at the thymidine kinase locus in diploid human lymphoblasts. *Mutat Res*. 94(2): 467-85.
- Lundblad, V. (2000). DNA ends: maintenance of chromosome termini versus repair of double strand breaks. *Mutat Res*. 451(1-2): 227-40.
- Makita, N., Kano, A., Yamayoshi, A., Akaike, T. and Maruyama, A. (2005). Modulation of highly ordered structures of human telomeric sequence by cationic copolymers. *Nucleic Acids Symp Ser (Oxf)*.(49): 53-4.
- Mathog, D., Hochstrasser, M., Gruenbaum, Y., Saumweber, H. and Sedat, J. (1984). Characteristic folding pattern of polytene chromosomes in *Drosophila* salivary gland nuclei. *Nature*. 308(5958): 414-21.
- Matsugami, A., Tsuchibayashi, H., Xu, Y., Noguchi, Y., Sugiyama, H. and Katahira, M. (2006). The new models of the human telomere DNA in K<sup>+</sup> solution revealed by NMR analysis assisted by the incorporation of 8-bromoguanines. *Nucleic Acids Symp Ser (Oxf)*.(50): 45-6.
- McKee, B. D. (2004). Homologous pairing and chromosome dynamics in meiosis and mitosis. *Biochim Biophys Acta*. 1677(1-3): 165-80.
- Merok, J. R., Lansita, J. A., Tunstead, J. R. and Sherley, J. L. (2002). Cosegregation of chromosomes containing immortal DNA strands in cells that cycle with asymmetric stem cell kinetics. *Cancer Res*. 62(23): 6791-5.
- Meyer-Ficca, M., Muller-Navia, J. and Scherthan, H. (1998). Clustering of pericentromeres initiates in step 9 of spermiogenesis of the rat (*Rattus norvegicus*) and contributes to a well defined genome architecture in the sperm nucleus. *J Cell Sci*. 111 ( Pt 10): 1363-70.
- Mudrak, O., Tomilin, N. and Zalensky, A. (2005). Chromosome architecture in the decondensing human sperm nucleus. *J Cell Sci*. 118(Pt 19): 4541-50.
- Nagele, R. G., Velasco, A. Q., Anderson, W. J., McMahon, D. J., Thomson, Z., Fazekas, J., Wind, K. and Lee, H. (2001). Telomere associations in interphase nuclei: possible role in maintenance of interphase chromosome topology. *J Cell Sci*. 114(Pt 2): 377-88.

- Neusser, M., Schubel, V., Koch, A., Cremer, T. and Muller, S. (2007). Evolutionarily conserved, cell type and species-specific higher order chromatin arrangements in interphase nuclei of primates. *Chromosoma*. 116(3): 307-20.
- Nugent, C. I. and Lundblad, V. (1998). The telomerase reverse transcriptase: components and regulation. *Genes Dev*. 12(8): 1073-85.
- Ohzeki, J., Nakano, M., Okada, T. and Masumoto, H. (2002). CENP-B box is required for de novo centromere chromatin assembly on human alphoid DNA. *J Cell Biol*. 159(5): 765-75.
- Okada, T., Ohzeki, J., Nakano, M., Yoda, K., Brinkley, W. R., Larionov, V. and Masumoto, H. (2007). CENP-B controls centromere formation depending on the chromatin context. *Cell*. 131(7): 1287-300.
- Oller, A. R., Buser, C. W., Tyo, M. A. and Thilly, W. G. (1989). Growth of mammalian cells at high oxygen concentrations. *J Cell Sci*. 94 ( Pt 1): 43-9.
- Orias, E. (1991). Evolution of amitosis of the ciliate macronucleus: gain of the capacity to divide. *J Protozool*. 38(3): 217-21.
- Pabo, C. O. and Sauer, R. T. (1984). Protein-DNA recognition. *Annu Rev Biochem*. 53: 293-321.
- Paeschke, K., Simonsson, T., Postberg, J., Rhodes, D. and Lipps, H. J. (2005). Telomere end-binding proteins control the formation of G-quadruplex DNA structures in vivo. *Nat Struct Mol Biol*. 12(10): 847-54.
- Parada, L. A., Roix, J. J. and Misteli, T. (2003). An uncertainty principle in chromosome positioning. *Trends Cell Biol*. 13(8): 393-6.
- Parkinson, G. N., Lee, M. P. and Neidle, S. (2002). Crystal structure of parallel quadruplexes from human telomeric DNA. *Nature*. 417(6891): 876-80.
- Paulson, J. R. and Laemmli, U. K. (1977). The structure of histone-depleted metaphase chromosomes. *Cell*. 12(3): 817-28.
- Potten, C. S., Owen, G. and Booth, D. (2002). Intestinal stem cells protect their genome by selective segregation of template DNA strands. *J Cell Sci*. 115(Pt 11): 2381-8.
- Prescott, D. M. (1994). The DNA of ciliated protozoa. *Microbiol Rev*. 58(2): 233-67.
- Probst, A. V. and Almouzni, G. (2008). Pericentric heterochromatin: dynamic organization during early development in mammals. *Differentiation*. 76(1): 15-23.
- Rambhatla, L., Ram-Mohan, S., Cheng, J. J. and Sherley, J. L. (2005). Immortal DNA strand



cosegregation requires p53/IMPDH-dependent asymmetric self-renewal associated with adult stem cells. *Cancer Res.* 65(8): 3155-61.

Rando, T. A. (2007). The immortal strand hypothesis: segregation and reconstruction. *Cell.* 129(7): 1239-43.

Rawlins, D. J. and Shaw, P. J. (1990). Localization of ribosomal and telomeric DNA sequences in intact plant nuclei by in-situ hybridization and three-dimensional optical microscopy. *J Microsc.* 157(Pt 1): 83-9.

Scherthan, H., Weich, S., Schwegler, H., Heyting, C., Harle, M. and Cremer, T. (1996). Centromere and telomere movements during early meiotic prophase of mouse and man are associated with the onset of chromosome pairing. *J Cell Biol.* 134(5): 1109-25.

Shinin, V., Gayraud-Morel, B., Gomes, D. and Tajbakhsh, S. (2006). Asymmetric division and cosegregation of template DNA strands in adult muscle satellite cells. *Nat Cell Biol.* 8(7): 677-87.

Skopek, T. R., Liber, H. L., Penman, B. W. and Thilly, W. G. (1978). Isolation of a human lymphoblastoid line heterozygous at the thymidine kinase locus: possibility for a rapid human cell mutation assay. *Biochem Biophys Res Commun.* 84(2): 411-6.

Slijepcevic, P., Xiao, Y. and Natarajan, A. T. (2000). Chromosome-specific telomeric associations in Chinese hamster embryonic cells. *Genes Chromosomes Cancer.* 28(1): 98-105.

Solov'eva, L., Svetlova, M., Bodinski, D. and Zalensky, A. O. (2004). Nature of telomere dimers and chromosome looping in human spermatozoa. *Chromosome Res.* 12(8): 817-23.

Sudo, H., Li-Sucholeiki, X. C., Marcelino, L. A., Gruhl, A. N., Zarbl, H., Willey, J. C. and Thilly, W. G. (2006). Distributions of five common point mutants in the human tracheal-bronchial epithelium. *Mutat Res.* 596(1-2): 113-27.

Sundquist, W. I. and Klug, A. (1989). Telomeric DNA dimerizes by formation of guanine tetrads between hairpin loops. *Nature.* 342(6251): 825-9.

Taddei, A. and Gasser, S. M. (2004). Multiple pathways for telomere tethering: functional implications of subnuclear position for heterochromatin formation. *Biochim Biophys Acta.* 1677(1-3): 120-8.

Tanabe, H., Habermann, F. A., Solovei, I., Cremer, M. and Cremer, T. (2002). Non-random radial arrangements of interphase chromosome territories: evolutionary considerations and functional implications. *Mutat Res.* 504(1-2): 37-45.

Tanabe, H., Muller, S., Neusser, M., von Hase, J., Calcagno, E., Cremer, M., Solovei, I., Cremer, C. and Cremer, T. (2002). Evolutionary conservation of chromosome territory arrangements in cell nuclei from higher primates. *Proc Natl Acad Sci U S A.* 99(7): 4424-9.

Tannenbaum, E., Sherley, J. L. and Shakhnovich, E. I. (2005). Evolutionary dynamics of adult stem cells: comparison of random and immortal-strand segregation mechanisms. *Phys Rev E Stat Nonlin Soft Matter Phys.* 71(4 Pt 1): 041914.

Ten Hagen, K. G., Gilbert, D. M., Willard, H. F. and Cohen, S. N. (1990). Replication timing of DNA sequences associated with human centromeres and telomeres. *Mol Cell Biol.* 10(12): 6348-55.

Trelles-Sticken, E., Dresser, M. E. and Scherthan, H. (2000). Meiotic telomere protein Ndj1p is required for meiosis-specific telomere distribution, bouquet formation and efficient homologue pairing. *J Cell Biol.* 151(1): 95-106.

Volpi, E. V., Chevret, E., Jones, T., Vatcheva, R., Williamson, J., Beck, S., Campbell, R. D., Goldsworthy, M., Powis, S. H., Ragoussis, J., Trowsdale, J. and Sheer, D. (2000). Large-scale chromatin organization of the major histocompatibility complex and other regions of human chromosome 6 and its response to interferon in interphase nuclei. *J Cell Sci.* 113 ( Pt 9): 1565-76.

Vorlickova, M., Chladkova, J., Kejnovska, I., Fialova, M. and Kypr, J. (2005). Guanine tetraplex topology of human telomere DNA is governed by the number of (TTAGGG) repeats. *Nucleic Acids Res.* 33(18): 5851-60.

Weierich, C., Brero, A., Stein, S., von Hase, J., Cremer, C., Cremer, T. and Solovei, I. (2003). Three-dimensional arrangements of centromeres and telomeres in nuclei of human and murine lymphocytes. *Chromosome Res.* 11(5): 485-502.

Wiblin, A. E., Cui, W., Clark, A. J. and Bickmore, W. A. (2005). Distinctive nuclear organisation of centromeres and regions involved in pluripotency in human embryonic stem cells. *J Cell Sci.* 118(Pt 17): 3861-8.

Wright, W. E., Tesmer, V. M., Huffman, K. E., Levene, S. D. and Shay, J. W. (1997). Normal human chromosomes have long G-rich telomeric overhangs at one end. *Genes Dev.* 11(21): 2801-9.

Wu, J. C. and Manuelidis, L. (1980). Sequence definition and organization of a human repeated DNA. *J Mol Biol.* 142(3): 363-86.

Xu, Y., Hirohata, Y. and Komiyama, M. (2007). Sequence-specific cleavage of human telomere DNA by G-quadruplex formation. *Nucleic Acids Symp Ser (Oxf.)*(51): 199-200.

Xu, Y., Noguchi, Y. and Sugiyama, H. (2006). The new models of the human telomere d[AGGG(TTAGGG)<sub>3</sub>] in K<sup>+</sup> solution. *Bioorg Med Chem.* 14(16): 5584-91.

Yang, T. P., Hansen, S. K., Oishi, K. K., Ryder, O. A. and Hamkalo, B. A. (1982). Characterization of a cloned repetitive DNA sequence concentrated on the human X

chromosome. *Proc Natl Acad Sci U S A.* 79(21): 6593-7.

Zalenskaya, I. A. and Zalensky, A. O. (2004). Non-random positioning of chromosomes in human sperm nuclei. *Chromosome Res.* 12(2): 163-73.

Zalensky, A. O., Allen, M. J., Kobayashi, A., Zalenskaya, I. A., Balhorn, R. and Bradbury, E. M. (1995). Well-defined genome architecture in the human sperm nucleus. *Chromosoma.* 103(9): 577-90.

Zalensky, A. O., Breneman, J. W., Zalenskaya, I. A., Brinkley, B. R. and Bradbury, E. M. (1993). Organization of centromeres in the decondensed nuclei of mature human sperm. *Chromosoma.* 102(8): 509-18.

Zalensky, A. O., Tomilin, N. V., Zalenskaya, I. A., Teplitz, R. L. and Bradbury, E. M. (1997). Telomere-telomere interactions and candidate telomere binding protein(s) in mammalian sperm cells. *Exp Cell Res.* 232(1): 29-41.

Zink, D. and Cremer, T. (1998). Cell nucleus: chromosome dynamics in nuclei of living cells. *Curr Biol.* 8(9): R321-4.

Zink, D., Cremer, T., Saffrich, R., Fischer, R., Trendelenburg, M. F., Ansorge, W. and Stelzer, E. H. (1998). Structure and dynamics of human interphase chromosome territories in vivo. *Hum Genet.* 102(2): 241-51.

Zirbel, R. M., Mathieu, U. R., Kurz, A., Cremer, T. and Lichter, P. (1993). Evidence for a nuclear compartment of transcription and splicing located at chromosome domain boundaries. *Chromosome Res.* 1(2): 93-106.